



UNIVERSITY OF LEEDS

This is a repository copy of *Investigation on liquid flow characteristics in microtubes*.

White Rose Research Online URL for this paper:

<http://eprints.whiterose.ac.uk/142502/>

Version: Accepted Version

---

**Article:**

Chen, Q-L, Wu, K-J [orcid.org/0000-0001-8658-5449](http://orcid.org/0000-0001-8658-5449) and He, C-H (2015) Investigation on liquid flow characteristics in microtubes. *AIChE Journal*, 61 (2). 2. pp. 718-735. ISSN 0001-1541

<https://doi.org/10.1002/aic.14656>

---

© 2014 American Institute of Chemical Engineers. This is the peer reviewed version of the following article: Chen, Q-L, Wu, K-J and He, C-H (2015) Investigation on liquid flow characteristics in microtubes. *AIChE Journal*, 61 (2). 2. pp. 718-735. ISSN 0001-1541, which has been published in final form at <https://doi.org/10.1002/aic.14656>. This article may be used for non-commercial purposes in accordance with Wiley Terms and Conditions for Use of Self-Archived Versions.

**Reuse**

Items deposited in White Rose Research Online are protected by copyright, with all rights reserved unless indicated otherwise. They may be downloaded and/or printed for private study, or other acts as permitted by national copyright laws. The publisher or other rights holders may allow further reproduction and re-use of the full text version. This is indicated by the licence information on the White Rose Research Online record for the item.

**Takedown**

If you consider content in White Rose Research Online to be in breach of UK law, please notify us by emailing [eprints@whiterose.ac.uk](mailto:eprints@whiterose.ac.uk) including the URL of the record and the reason for the withdrawal request.



[eprints@whiterose.ac.uk](mailto:eprints@whiterose.ac.uk)  
<https://eprints.whiterose.ac.uk/>

# Investigation on liquid flow characteristics in microtubes

*Qiao-Li Chen, Ke-Jun Wu\*, Chao-Hong He*

State Key Laboratory of Chemical Engineering, Department of Chemical and Biological Engineering,  
Zhejiang University, Hangzhou 310027, China

\* corresponding author, fax: + 86 571 87951742, tel.: + 86 571 87952709, e-mail: [wkj@zju.edu.cn](mailto:wkj@zju.edu.cn).

Abstract: The fundamental understanding and prediction of liquid flow characteristics in microscale are important to control the performance of microfluidic devices. However, fundamental questions about liquid flow characteristics in microscale have not been settled yet and systematical investigation is needed. A systematical investigation on liquid flow characteristics through microtubes with diameters varying from 44.5-1011  $\mu\text{m}$  and relative roughness in the range 0.02-4.32% in the Reynolds number range 29-11644 was performed in this work, using water as working fluid. Experimental results indicated that early transition occurred when the diameter was smaller than 1000  $\mu\text{m}$ , the transitional flow characteristics for smooth microtubes differed from rough microtubes and the friction factor in turbulent region for rough microtubes was larger than conventional theory. Moreover, a parameter  $\alpha$  was proposed to describe the characteristic of microtube. The characteristic parameter was used to calculate the critical Reynolds number and the friction factor in turbulent region for microscale.

Topical Heading: Transport Phenomena and Fluid Mechanics

Keywords: microfluidic, microtube, liquid flow characteristics, critical Reynolds number, friction factor

## 1 **1 Introduction**

2       Microscale systems have attracted much attention of researchers<sup>1-8</sup> and are believed to play an  
3 important role in chemical processes. The fundamental understanding and prediction of the liquid flow  
4 characteristics in microscale are important to control the performance of microfluidic devices. A large  
5 number of experimental investigations focus on liquid flow characteristics in microscale have been  
6 reported and a brief overview of these researches has been presented in the most recent reviews.<sup>9-12</sup> As  
7 can be found in these reviews, the liquid flow characteristics in microscale different researchers  
8 observed are inconsistent. Besides, among all the experimental studies,<sup>9-12</sup> studies of laminar flow  
9 characteristics are mostly addressed while studies of transitional and turbulent flow characteristics  
10 seem to be in a lack. The fundamental liquid flow characteristics for the whole flow regions in  
11 microscale are still unclear.

12       The flow characteristics were usually quantitatively analyzed based on the Reynolds number and  
13 friction factor in literature. To understand the liquid flow characteristics, there are four basic questions  
14 to be explored. 1) Whether the friction factor of laminar flow in microscale is still the same as  
15 conventional theory? Will it be affected by the decrease of diameter, increase of roughness or other  
16 factors? 2) Can early transition, which means early departure from laminar flow (lower critical  
17 Reynolds number than conventional theory), be observed in microscale? If the answer is yes, then  
18 what is the cause of early transition? 3) Is there any difference between the transitional flow  
19 characteristic in microscale and that in conventional scale? 4) Whether the friction factor of turbulent  
20 flow in microscale can be predicted by conventional theory.

21       There are about a hundred references related to microscale flows that have discussed question

1 one. The most representative ones are listed in this paragraph. Peng et al.<sup>13</sup> and Jiang et al.<sup>14</sup> found that  
2 smaller channels had lower friction factor (in laminar flow region), while Mala et al.<sup>15</sup> reported that as  
3 the Reynolds number increased, a significant positive deviation from the conventional theory was  
4 observed and the deviation increased as the microtube diameter decreased. Some other researchers<sup>16-19</sup>  
5 also observed higher friction factor (in laminar flow region). However, most recently, researchers<sup>20-25</sup>  
6 generally agreed that friction factor (in laminar flow region) fitted well with conventional theory  
7 within experimental uncertainties. The details about the references mentioned above are listed in Table  
8 1.

9 A lot of references mentioned critical Reynolds number in their study though not as much as  
10 those focused on laminar flow. However, fewer references gave specific values of critical Reynolds  
11 number according to different dimensions (such as diameters or roughnesses) of microtubes (or  
12 microchannels) and even limited number of references gave further discussion on critical Reynolds  
13 number. Some researchers<sup>26-29</sup> found that the critical Reynolds number was around 1800-2000 and  
14 considered that the same as conventional theory. However, most researchers<sup>13,17,18,30-38</sup> thought that  
15 early transition exists. Broadly speaking, there are two views on the cause of early transition. One  
16 view is that the decrease of diameter leads to an occurrence of early transition. Peng et al.<sup>13</sup> found that  
17 the laminar flow transition occurred at Reynolds number in the range of 200-700 and the critical  
18 Reynolds number was strongly affected by the hydraulic diameter. Pfund et al.<sup>17</sup> also found that the  
19 critical Reynolds number decreased further with decreasing channel depth. However, the critical  
20 Reynolds number values they observed were much larger than the values of 200-700. In some other  
21 studies,<sup>34,38</sup> they listed the specific values of critical Reynolds number of each microtube and proposed

1 the same conclusion as Peng et al.<sup>13</sup> and Pfund et al.<sup>17</sup> that the smaller the microtube diameter, the  
2 lower the critical Reynolds number. The other view is that the increase of roughness leads to lower  
3 critical Reynolds number in microscale. Tang et al.<sup>35</sup> observed that the transition from laminar to  
4 turbulent flow occurred earlier and attributed the result to surface roughness effect. Kandlikar et al.<sup>36</sup>  
5 also suggested that the laminar to turbulent transition was seen to occur at lower Reynolds number  
6 with an increase in the roughness. In their later work,<sup>37</sup> they did more experiments to support their  
7 conclusion. The details about the references mentioned above are listed in Table 2.

8 Only a few reports discussed the liquid flow characteristic in the transitional flow region. Almost  
9 all the related references are listed in this paragraph. Some researchers<sup>28,30,39-42</sup> thought that the  
10 transitional flow region in microscale could be regarded as the same as conventional theory though the  
11 specific Reynolds number ranges of transition flow they observed were different. Some researchers  
12 observed different transitional flow characteristics in microscale as compared with conventional scale  
13 and thought that it was caused by the effect of roughness. Bucci et al.<sup>43</sup> found that the smallest  
14 microtube (diameter 172  $\mu\text{m}$ ) with the highest value of relative roughness (0.87%) showed a “rough”  
15 laminar to turbulent flow transition while the other two microtubes showed a “smooth” laminar to  
16 turbulent flow transition (“rough” meant that the friction factor in the transitional region increased  
17 quickly as the Reynolds number increased and “smooth” meant that the friction factor in the  
18 transitional region increased slowly as the Reynolds number increased). They attributed this effect to  
19 the increase of surface roughness. Barlak et al.<sup>25</sup> noticed “smooth” and “rough” transition for different  
20 microtubes, too. Some other researchers observed different transitional flow characteristics in  
21 microscale, but thought that it was due to the decrease of diameter. Yang et al.<sup>44</sup> found that the

1 transition Reynolds number varied from 1200 to 3800 and increased with decreasing microtube  
2 diameter. Ghajar et al.<sup>38</sup> held the opinion that the Reynolds number range for transition flow became  
3 narrower with the decrease in microtube diameter. Moreover, Ghajar et al.<sup>38</sup> observed that further  
4 decrease in the microtube diameter from 667 to 337  $\mu\text{m}$  caused the transition Reynolds number  
5 shifting from 3000 to 1700, which was lower than conventional theory. The details about the  
6 references mentioned above are listed in Table 3.

7 With respect to question four, the number of related references is also limited. Almost all the  
8 related references are listed in this paragraph. Large diversities exist between different references.  
9 Hegab et al.<sup>39</sup> observed that the friction factor was lower than that predicted by commonly used  
10 conventional scale correlations<sup>45</sup> for flows in the turbulent region. Bucci et al.<sup>43</sup> and some other  
11 researchers<sup>28,44</sup> found that the friction factor (in turbulent flow region) agreed well with conventional  
12 scale correlations.<sup>46,47</sup> However, Celata et al.<sup>40</sup> found that the friction factor (in turbulent flow region)  
13 was higher than that predicted by Blasius equation<sup>47</sup> but lower than that by the Colebrook equation<sup>46</sup>  
14 with the experimental value of relative roughness. Agostini et al.<sup>26</sup> also found that the friction factor  
15 (in turbulent flow region) was higher than that predicted by Blasius equation.<sup>47</sup> Kandlikar et al.<sup>36</sup>  
16 found that the friction factor (in turbulent flow region) was considerably above the constant value  
17 obtained according to Miller equation.<sup>48</sup> Hrnjak and Tu<sup>21</sup> found that the friction factor (in turbulent  
18 flow region) followed Churchill's equation<sup>49</sup> with  $\varepsilon D_h^{-1}$  of about 0.7%, 0.5%, 2.0% and 0.3% for test  
19 section with  $\varepsilon D_h^{-1}$  of 0.16%, 0.14%, 0.35% and 0.29%, respectively. The details about the references  
20 mentioned above are listed in Table 4.

21 To sum up, these basic questions have not been settled yet and systematical investigation is

1 needed. While not attempting to answer these questions with surprising new findings, we tried to  
2 review the experimental results in literature, eliminate some confusion by carefully identifying and  
3 controlling experimental methods, systematically and quantitatively answer these questions based on  
4 the experimental data in this work and literature. Circular microtubes were used in this work and  
5 deionized degassed water was used as working fluid. Experiments were carried out to study the  
6 laminar, transitional, and turbulent flow characteristics of water in 20 different microtubes with  
7 Reynolds number ranging from 29-11644, especially focused on the critical Reynolds number and  
8 friction factor in turbulent flow. Flow characteristics in three types namely 316 stainless steel (SS),  
9 poly-ether-ether-ketone (PEEK), and fused silica (FS) of microtubes with their diameters ranging from  
10 44.5-1011  $\mu\text{m}$  and roughness (relative roughness) varying from 0.1-5.2  $\mu\text{m}$  (0.02-4.32%) have been  
11 studied. The major objectives of this work are to conduct accurate measurements in test section and  
12 answer the four basic questions, especially the questions about critical Reynolds number and friction  
13 factor in turbulent flow region, quantitatively.

## 14 **2 Experimental Setup**

### 15 2.1 Experimental apparatus

16 The experimental apparatus was designed to be accurate and versatile, which accommodated the  
17 use of multiple diameters and lengths of tested microtubes. The apparatus consists of two major  
18 components, including pressure system and test section. The overall schematic for the apparatus is  
19 presented in Figure 1.

20 The pressure system is comprised of a high pressure nitrogen cylinder (Jingong Air Co., Ltd.), a  
21 316 stainless steel buffer tank (max working pressure 6.4 MPa, volume 3 L), a 316 stainless steel fluid

1 reservoir (max working pressure 6.4 MPa, volume 9 L) and a constant temperature bath (Shanghai  
2 Rongfeng 501A). The liquid is pressurized either by a compressed, inert gas or a pump in literature.<sup>50</sup>  
3 The high pressure nitrogen cylinder is chosen as the pressure source in this work since it is a stable  
4 pressure source, indissolvable in water, and preferred by researchers.<sup>19,24,25,28,30,35,38,41,51-53</sup> The high  
5 purity nitrogen in the high pressure cylinder is pressurized to approximate 17 MPa by the distributor.  
6 Two precise nitrogen regulators are used to control the pressure of nitrogen inlet to the buffer tank  
7 (which is designed for the purpose of providing more stable pressure), one (Shanghai Regulator Co.,  
8 Ltd., YQD-6) is capable of providing pressures ranging from 0-1.6 MPa and another one (Linhai  
9 Pressure Gauge Co., Ltd., 370) is capable of providing pressures ranging from 0-6 MPa. A 2  $\mu\text{m}$   
10 microfilter (Beijing Xiongchuan Valves Manufacture Co., Ltd., SS-2210-3) is placed before the buffer  
11 tank to make sure that no dust enters the tank. It is possible that the dissolved gas in water will be  
12 released under high pressures and influence the flow characteristics. Thus, the deionized water is  
13 degassed and stored in the air-tight reservoir. The reservoir and test section are connected by a 316  
14 stainless steel tube (inner diameter 3 mm) which is wound into a series of circles and immersed into  
15 the constant temperature bath. The end of the tube (between the constant temperature bath and test  
16 section) is covered with thick thermal insulating foam. As the stable nitrogen is fed into the reservoir,  
17 the water is forced to flow through the constant temperature bath and then enter the test section.

18 The test section contains the test microtube as well as the equipments which are necessary for the  
19 measurement of inlet and outlet temperatures, pressure drop and mass flow rate. Another 2  $\mu\text{m}$   
20 microfilter (Beijing Xiongchuan Valves Manufacture Co., Ltd., SS-223-3) is placed before the test  
21 section to eliminate any particles and break bubbles. Three types of test microtubes are used in this

1 study, SS microtube (Valco Instruments Co., Inc.), PEEK microtube (Valco Instruments Co., Inc.),  
2 and FS microtube (SGE Analytical Science Pty., Ltd.). The diameters of these microtubes vary from  
3 44.5-1011  $\mu\text{m}$ . To testify the experimental phenomenon, some microtubes with similar diameters are  
4 used. At the inlet and outlet of the tested microtube, two sumps are fabricated to connect the tube. As  
5 mentioned in our previous work,<sup>54</sup> any insertion type measurement methods have an effect on the flow  
6 characteristics in the microtube. It is a difficult task to measure the fluid temperature in a microtube.  
7 Thus, in our work as well as some other studies in the literature,<sup>51,55-58</sup> sumps are used to install  
8 thermal resistances and pressure transducer. The detailed structure of the sumps can be found in our  
9 previous work.<sup>54</sup> The sumps and test microtubes are covered with thick thermal insulating foam. Two  
10 Pt100 resistance temperature detectors (RTDs, SMWZPM-201) with an accuracy of  $\pm 0.1$  K are  
11 embedded at the inlet and outlet sumps to measure the inlet and outlet temperatures of the fluid. The  
12 data is acquired from the resistance temperature detectors via a digital acquisition system (Advantech,  
13 USB 4718) and recorded using a computer. The max difference between inlet and outlet temperatures  
14 is less than 1 K. Thus, the average of the inlet and outlet temperatures is used to represent the fluid  
15 temperature just as the literature.<sup>33,35,57,59-62</sup> A pressure transducer (Rosemount 2051T) with an  
16 accuracy of 0.075% is embedded at the inlet sump to measure the inlet pressure. Since the outlet  
17 pressure is kept at the atmospheric pressure (the outlet sump is connected to the atmosphere), the inlet  
18 pressure value equals the pressure drop across the microtube. Thus, the value of inlet pressure is used  
19 to represent the pressure drop along the microtube as well as other references.<sup>18,57,59,63</sup> Both the  
20 resistance temperature detectors and pressure transducer are calibrated. When the experiment begins,  
21 particular attention is paid to remove air from the whole test section, especially the two sumps

1 (trapped air will influence the measurement of temperatures and pressures). Then, when the pressure  
2 and temperature values do not change any further, the flow is considered to have reached a steady  
3 state. A conical flask is used to collect the water from the outlet sump for certain minutes or seconds  
4 and an analytical balance (Shanghai Precision Scientific Instrument Co., Ltd., JA5003B) with an  
5 accuracy of 0.001g is used to measure the mass of the collected water. There shows no detectable  
6 evaporation for water during the collecting period, which is consistent with references<sup>18,19,30,32,57,59,63-67</sup>  
7 that have applied the same method. The ratio of mass to time is the mass flow rate.

## 8 2.2 Dimensions of microtubes

9 There are totally 20 microtubes which have been tested, including 13 SS microtubes (120.3-1011  
10  $\mu\text{m}$ ), 6 PEEK microtubes (44.5-530  $\mu\text{m}$ ), and 1 FS microtube (256  $\mu\text{m}$ ). The details of the dimensions  
11 of all the tested microtubes are listed in Table 5. A vernier caliper with a precision of 0.02 mm is used  
12 to measure the length of microtubes with their length less than or equals 200 mm and a meter ruler  
13 with a precision of 0.5 mm is used to measure the length of microtubes with their length larger than  
14 200 mm.

15 The precise measurement of microtube diameter is one of the most significant factors that  
16 determine the accuracy of this work. Technically, it is impossible to measure the “real” diameter  
17 directly. Researchers adopted different methods to obtain an approximate value of the diameter.  
18 Weight method can be used to obtain the average diameter along the microtube. Yang et al.<sup>44</sup> used  
19 weight method for tubes larger than 1.1 mm. They filled mercury into the tube and measured the  
20 weight of the mercury (the weight difference between the tube with mercury inside and the tube) to  
21 obtain the volume of the mercury. Then the average diameter could be obtained according to the

1 length of tube. There are several factors that contribute to the uncertainty in diameter measurement  
2 with weight method. The most important factor is the fill of mercury. Considering the fact that it is  
3 more difficult to fully fill mercury into smaller microtubes, the weight method may be less accurate  
4 for microtubes with smaller diameter. Besides, the mercury weight and density will also have effect on  
5 the accuracy of diameter measurement. Krishnamoorthy and Ghajar<sup>68</sup> (published in 2007) concluded  
6 that almost 15 out of 23 researchers used scanning electron microscope (SEM) method for accurate  
7 diameter measurement. As for the studies reported after 2007, almost all the researchers used SEM  
8 method to measure microtube diameter. SEM method utilizes a scanning electron microscope to  
9 obtain the image of cross section of the microtube (with a known pixel-to-length scale on the image).  
10 Then the SEM measurement software is used to calculate the diameter according to the scale. The  
11 uncertainty in diameter measurement with SEM method is also comprised of several contributions.  
12 First, the SEM itself owns a measurement uncertainty. Then, the diameter obtained through the SEM  
13 method can only represent the diameter of one cross section instead of an average value. The accuracy  
14 of diameter value can be affected if the diameter varies along the microtube. Moreover, there may be  
15 some human bias in the calculation, which is difficult to quantify. Thus, as much as possible  
16 calculations on one image should be performed to diminish the human bias as far as possible.

17 In our previous work,<sup>54,69,70</sup> we have performed experiments (comparison between the diameters  
18 measured by the weight method and SEM method) for microtubes with diameter larger than 250  $\mu\text{m}$   
19 to verify that the diameters can be assumed to be uniform along the microtube. Hence, SEM method is  
20 used in this work and only the diameters of both ends of the microtubes are measured in this work,  
21 just the same as some other studies in the literature.<sup>59,60,71</sup> A Thermal Field Emission Scanning

1 Electron Microscope (FEI, SIRION-100) is used to measure the diameters of microtubes. A  
2 verification regulation for analytical scanning electron microscope (JJG Education Office 010-1996) is  
3 acquired to calibrate the SEM using the same SEM acceleration voltage and magnifications as that  
4 used for the diameter measurement of microtubes. The accuracy of the SEM is found to be around  
5 0.5%. All the microtubes are washed in an ultrasonic cleaner before the measurement. The PEEK  
6 microtubes are sputter-coated with gold to be electric and make sure that clear images of diameters are  
7 obtained. Once images of diameters have been captured, the SEM software is used to calculate the  
8 diameter. The diameter images of one end of tested microtubes SS1011 (SS stands for the material of  
9 microtube and 1011 stands for the diameter of microtube, similarly hereinafter), SS523, PEEK530,  
10 and PEEK75.3 are shown in Figure 2 and all the diameter images of both ends of the 20 tested  
11 microtubes are shown in the supporting information Figure S1. Ten calculations of one image are  
12 averaged to minimize the human bias. As can be observed in Table 5, the max deviation of the  
13 diameters for the two ends is 0.9% and the average absolute deviation for all microtubes is 0.3%. Thus,  
14 the average diameter of the two ends (twenty calculations) is calculated to represent the diameter of  
15 the microtube just as other literature.<sup>59,60,71</sup> The precision of the diameter values obtained in this work  
16 is around 1.00% considering all the contributions.

17 An optical profiler (Veeco Instruments Inc., Wyko NT9100, precision  $\pm 0.1 \mu\text{m}$ ) which is capable  
18 of non-contact, three-dimensional measurements is used to measure the surface roughness of  
19 microtubes. Average roughness ( $R_a$ ) and root mean square roughness ( $R_q$ ) can be obtained. According  
20 to references,<sup>20,21,62,71-73</sup> average roughness ( $R_a$ ) is chosen to represent the roughness ( $\varepsilon$ ) of microtubes.  
21 The microtubes are sanded for the purpose of having their inner surface revealed and then washed in

1 an ultrasonic cleaner before the measurement. PEEK and FS microtubes can be easily obtained and  
2 are always regarded as smooth microtubes in literature.<sup>17,21,27,57,74-76</sup> Thus, only 2 pieces of 6 PEEK  
3 microtubes are chosen to have the roughness measured and measurements are taken from four  
4 different sections of each microtube. The value of the measured roughness of PEEK microtubes is in  
5 the range 0.0-0.2  $\mu\text{m}$  and is averaged to 0.1  $\mu\text{m}$ , which is in accordance with the literature value.<sup>17,21</sup>  
6 For the roughness of FS microtube, literature value<sup>27,57,74,75</sup> is in the range 0-70 nm. So the roughness  
7 of FS microtube is rounded to 0.1  $\mu\text{m}$  in this work. As for the 13 SS microtubes, surface roughnesses  
8 are taken from six different sections of each microtube. The detailed roughness images of every  
9 section of 13 SS and 2 PEEK microtubes are shown in supporting information Figure S2. The average  
10 roughness of each microtube is listed in Table 5 and the roughness images of one section of tested  
11 microtubes SS1011, SS523, SS120.3, and PEEK530, are shown in Figure 3.

### 12 2.3 Mathematical formulations

13 The fluid temperature ( $T$ ), pressure drop ( $\Delta P$ ), and mass flow rate ( $M$ ) are obtained through the  
14 experiment. The density ( $\rho$ ) and viscosity ( $\eta$ ) of water are calculated according to fluid temperature.

15 Thus, the Reynolds number (Re) can be calculated as follow

$$16 \text{Re} = \frac{4M}{\pi\eta D} \quad (1)$$

17 The friction factor ( $f$ ) can be obtained according to equation 2

$$18 f = \frac{\Delta P_{\text{FD}} \pi^2 D^4 \rho D}{8M^2 L} \quad (2)$$

19 where  $\Delta P_{\text{FD}}$  is fully developed flow pressure drop and can be calculated as

1  $\Delta P_{FD} = \Delta P - \Delta P_{in} - \Delta P_D - \Delta P_{out}$  (3)

2 where  $\Delta P_{in}$  is pressure losses due to the abrupt contraction in the inlet,  $\Delta P_D$  is pressure losses in  
3 hydrodynamic development flow (unfully developed flow in the entrance part), and  $\Delta P_{out}$  is pressure  
4 losses due to the abrupt extension in the outlet.  $\Sigma K_L$  is used to represent the additional pressure losses  
5 as follow<sup>18,19,35,41,52,53,55,57-60,77</sup>

6  $\Delta P_{in} + \Delta P_D + \Delta P_{out} = \Sigma K_L \frac{8M^2}{\pi^2 D^4 \rho}$  (4)

7 Combining equations 2, 3 and 4, friction factor can be calculated as

8  $f = \left( \frac{\Delta P \pi^2 D^4 \rho}{8M^2} - \Sigma K_L \right) \frac{D}{L}$  (5)

9 where  $\Sigma K_L$  can be expressed in different ways. Different references<sup>18,19,35,41,52,53,55,57-60,77</sup> gave different  
10 expressions of  $\Sigma K_L$ . For example, Li et al.<sup>18,57</sup> suggested that  $\Sigma K_L$  equaled 2.36, Judy et al.<sup>59</sup> pointed  
11 out that  $\Sigma K_L$  equaled 3.1, and Ergu et al.<sup>19</sup> thought that  $\Sigma K_L$  should be calculated by a complex  
12 expression. Since it is difficult to define a specific value of  $\Sigma K_L$ , some researchers proposed other  
13 methods to eliminate the additional pressure losses. Researchers<sup>17,66,67,72</sup> who used wide channels  
14 placed pressure taps far away from the inlet and outlet for the purpose of measuring the pressure drop  
15 of fully developed flow directly. However, it is difficult for microtubes to copy this method without  
16 disrupting the flow.<sup>24,65</sup> Some other researchers<sup>15,24,43,64,65</sup> utilized a short and a long microtube method.  
17 Thus,  $(\Delta P_{long} - \Delta P_{short})$  represents the pressure drop of fully developed flow over the tube length ( $L_{long} -$   
18  $L_{short}$ ). However, it is impossible to find a short and a long microtube sharing the exactly same  
19 diameter and surface roughness. Even the microtubes which are bought in a same batch from a same  
20 corporation will not be accurately uniform. In a word, it is impossible to find a perfect method which

1 could totally eliminate errors. Thus, we choose to follow the most simple and typical  
 2 method,<sup>35,53,55,58,78</sup> i.e., perform experiments in long enough microtubes to neglect the hydrodynamic  
 3 development flow and define that

$$4 \quad \Delta P_{\text{in}} + \Delta P_{\text{out}} = 1.5 \frac{8M^2}{\pi^2 D^4 \rho} \quad (6)$$

5 Thus, equation 5 can be simplified to equation 7

$$6 \quad f = \left( \frac{\Delta P \pi^2 D^4 \rho}{8M^2} - 1.5 \right) \frac{D}{L} \quad (7)$$

7 and Poiseuille number ( $f\text{Re}$ ) can be expressed as

$$8 \quad f \text{Re} = \left( \frac{\Delta P \pi^2 D^4 \rho}{8M^2} - 1.5 \right) \frac{4M}{L\pi\eta} \quad (8)$$

#### 9 2.4 Uncertainty analysis

10 Understanding the experimental uncertainty of calculated Reynolds number ( $\text{Re}$ ), friction factor  
 11 ( $f$ ), and Poiseuille number ( $f\text{Re}$ ) is necessary. According to uncertainty calculation method<sup>59,79</sup> and  
 12 equations 1, 7 and 8, the uncertainty in  $\text{Re}$ ,  $f$ , and  $f\text{Re}$  can be expressed as

$$13 \quad \frac{\delta \text{Re}}{\text{Re}} = \left[ \left( \frac{\delta M}{M} \right)^2 + \left( \frac{\delta \eta}{\eta} \right)^2 + \left( \frac{\delta D}{D} \right)^2 \right]^{1/2} \quad (9)$$

$$14 \quad \frac{\delta f}{f} = \left[ \left( \frac{\delta \Delta P}{\Delta P} \right)^2 + \left( 5 \frac{\delta D}{D} \right)^2 + \left( \frac{\delta \rho}{\rho} \right)^2 + \left( 2 \frac{\delta M}{M} \right)^2 + \left( \frac{\delta L}{L} \right)^2 \right]^{1/2} \quad (10)$$

$$15 \quad \frac{\delta f \text{Re}}{f \text{Re}} = \left[ \left( \frac{\delta M}{M} \right)^2 + \left( \frac{\delta \eta}{\eta} \right)^2 + \left( 4 \frac{\delta D}{D} \right)^2 + \left( \frac{\delta \Delta P}{\Delta P} \right)^2 + \left( \frac{\delta \rho}{\rho} \right)^2 + \left( \frac{\delta L}{L} \right)^2 \right]^{1/2} \quad (11)$$

16 where  $\delta M/M$ ,  $\delta \eta/\eta$ ,  $\delta D/D$ ,  $\delta \Delta P/\Delta P$ ,  $\delta \rho/\rho$ , and  $\delta L/L$  mean uncertainty in mass flow rate, viscosity,  
 17 diameter, pressure drop, density and length. Attempts have been made to reduce the experimental  
 18 uncertainty in these items as far as possible. A detailed description of the contributions to the

1 uncertainty in diameter is given above and the uncertainty is approximately 1%. The uncertainty in  
2 mass flow rate results from the 0.001g uncertainty in mass and human bias in timekeeping, and is  
3 estimated to be less than 0.1%. The uncertainties in viscosity and density result from 0.1-0.5 K  
4 uncertainty in temperature and are estimated to be less than 1% and 0.01%, respectively. The  
5 uncertainty in pressure drop is given by the manufacturer and the uncertainty in length is determined  
6 by the vernier caliper and meter ruler. The details of uncertainty are listed in Table 6.

### 7 **3 Results and Discussion**

#### 8 3.1 Experimental results

9 The experimental results of  $f$  vs  $Re$  relationship (in the log-log plot) for tested microtubes SS1011,  
10 SS523, SS120.3, and PEEK140.5 are shown as representative in Figure 4 (results of all the 20 tested  
11 microtubes are shown in supporting information Figure S3). On the whole, the tendency of  $f$  vs  $Re$   
12 relationship for microtubes is approximately the same as conventional sized tubes. In the laminar flow  
13 region ( $Re < Re_c$ ,  $Re_c$  is the critical Reynolds number), the friction factor decreases linearly with the  
14 increase of Reynolds number (in the log-log plot) and the Poiseuille number keeps constant as  
15 Reynolds number increases. At critical Reynolds number ( $Re = Re_c$ ), a transition from laminar to  
16 turbulent flow starts. After that,  $f$  vs  $Re$  relationship (in the log-log plot) is not in linear relation  
17 anymore and the Poiseuille number rises with the increase of Reynolds number ( $Re_c < Re < Re_t$ ,  $Re_t$  is  
18 the Reynolds number where turbulent flow begins). Attention should be paid that the critical Reynolds  
19 number is defined as the point that friction factor starts to deviate from the linear portion of  $f$  vs  $Re$   
20 plot in laminar flow region, i.e. the point that Poiseuille number begin to rise with the increase of  
21 Reynolds number, in the present work as well as other literature,<sup>17,18,33,34,36-38</sup> not the point that friction

1 factor starts to increase as the increase of Reynolds number. When the Reynolds number becomes  
2 larger ( $Re > Re_t$ ), the friction factor decreases slowly with the increase of Reynolds number. This is  
3 the turbulent flow region. Similarly, the experimental results of other tested microtubes can be divided  
4 into the three regions, the laminar flow region, transitional flow region and turbulent flow region. As  
5 can be observed in Figure 4, for the microtubes with diameter  $\geq 140.5 \mu\text{m}$ , laminar, transitional, and  
6 turbulent flows are studied, while for microtubes with diameter  $< 140.5 \mu\text{m}$ , the current experimental  
7 facility and methods limit the experimental Reynolds number to be less than 2280 and only laminar  
8 and beginning of transitional flows are studied.

9 A total of 2502 data points (687, 1277 and 538 data points for laminar, transitional, and turbulent  
10 flow, respectively) were obtained over the Reynolds number range 29-11644 (the detailed data which  
11 include density ( $\rho$ ) and viscosity ( $\eta$ ) of water, mass flow rate ( $M$ ), pressure drop ( $\Delta P$ ), Reynolds  
12 number ( $Re$ ), friction factor ( $f$ ), and Poiseuille number ( $fRe$ ) of 2502 data points for all the 20 tested  
13 microtubes are listed in supporting information Tables S1-20). The experimental results as well as  
14 ranges of experimental Reynolds number ( $Re$ ), ranges of experimental friction factor ( $f$ ), average  
15 Poiseuille number ( $fRe$ ) of laminar flow, critical Reynolds number ( $Re_c$ ), and Reynolds number where  
16 turbulent flow begins ( $Re_t$ ) are listed in Table 7. Differences of liquid flow characteristics between  
17 microtubes and conventional sized tubes can be observed from Table 7. The flow characteristics are  
18 discussed in detail in the following passages.

### 19 3.2 Laminar flow region

20 The experimental results of  $f$  vs  $Re$  relationship of all the tested microtubes in the laminar flow  
21 region are shown in supporting information Figure S3. The experimental friction factor and Reynolds

1 number have an almost linear trend as predicted by the conventional theory of Hagen-Poiseuille for  
2 the laminar flow. The corresponding enlargement of experimental results of  $fRe$  vs  $Re$  plot of all the  
3 tested microtubes in laminar flow region are shown in Figure 5. The experimental values of Poiseuille  
4 number are seen to keep constant as Reynolds number increases (in the laminar flow region) within  
5 measurement error. For each tested microtube, the average of all the Poiseuille number in laminar flow  
6 region ( $(fRe)_{\text{laminar,ave}}$ ) is calculated and listed in Table 7. Almost all the laminar flow data nicely lay  
7 next to the average value 64. This finding is in accordance with the recent researches.<sup>20-25</sup> Therefore,  
8 conclusion can be made that to the degree of the current experimental uncertainties, the Poiseuille  
9 number values agree well with theoretical predictions ( $fRe$  equals the constant 64) for microtubes with  
10 diameters in the range 44.5-1011  $\mu\text{m}$  and roughness (relative roughness) less than 5.2  $\mu\text{m}$  (4.32%).

### 11 3.3 Critical Reynolds number

12 Critical Reynolds number is the indicator of the transition from laminar to turbulent flow and the  
13 investigation on critical Reynolds number is meaningful. Researches on critical Reynolds number  
14 goes back to 1883 when Osborne Reynolds found that a laminar flow becomes unstable if the  
15 dimensionless number (which is named after him now) exceeds a certain critical value. However, due  
16 to the complexity of fluid dynamics, his finding still has not been explained satisfactorily by  
17 theory,<sup>80,81</sup> and research on the critical Reynolds number mainly relies on experimental results. In this  
18 work, a systematic experimental study of the critical Reynolds number was performed in various  
19 microtubes, the effects of microtube diameter and roughness on critical Reynolds number were also  
20 discussed.

21 To figure out whether early transition occurs in microtubes and what is the cause of early

1 transition, the specific value of critical Reynolds number should be first obtained using an appropriate  
2 mathematical method. Unfortunately, most of the references<sup>13,18,30-35</sup> did not mention how they  
3 obtained the values of critical Reynolds number. A few references<sup>37,38</sup> considered the Reynolds  
4 number where the deviation from the linear portion of the  $f$  vs Re in the log-log plot achieved some  
5 certain values, such as 1%<sup>37</sup> or 5%,<sup>38</sup> as the critical Reynolds number. It seems like that the deviation  
6 criterion is difficult to determine. In that case, a specific definition to calculate critical Reynolds  
7 number was proposed in this work.

8 Figure 5 shows the experimental results of  $fRe$  vs Re relationship in laminar flow region and  
9 beginning of transitional flow region for all the 20 tested microtubes. As can be observed in Figure 5,  
10 the Poiseuille number keeps constant as the increase of Reynolds number in laminar flow region. Then,  
11 the Poiseuille number increases with the increase of Reynolds number when the Reynolds number is  
12 larger than critical Reynolds number. The tendency of  $fRe$  vs Re relationship after critical Reynolds  
13 number is different from that before critical Reynolds number. Since the Poiseuille number is a  
14 continuous function of Reynolds number, the critical Reynolds number should be located on the  
15 crossing point of two trend lines. The calculation process of critical Reynolds number of SS1011 is  
16 given as an example (shown in Figure 5). Firstly, the approximate location of the critical Reynolds  
17 number is obtained and it is among 1800-2200 for SS1011 (the deviation of  $fRe$  from the Poiseuille  
18 number in laminar flow region 64 is larger than the uncertainty 4.13% among 1800-2200). Secondly,  
19 line 1 (horizontal line:  $fRe$  = average value of Poiseuille number in laminar flow region) which  
20 represents the tendency of the data in laminar flow region is obtained. Thirdly, line 2 (a linear  
21 regression line of the data points which are larger than 2200) which represents the tendency of the

1 beginning of transitional  $f/Re$  vs  $Re$  relationship is obtained. Finally, the crossing point of the two lines  
2 represents the value of critical Reynolds number. The deviation between the linear regression  
3 equations and experimental data is in the range 0.3-1.1% and the AAD was found to be 0.6% for all  
4 the 20 tested microtubes. Thus, considering the uncertainty in experiment and calculation method, the  
5 uncertainty in critical Reynolds number is approximately 2%.

6 The calculation results, two lines and their crossing point, for all the 20 tested microtubes are also  
7 shown in Figure 5. The specific values of critical Reynolds number are listed in Table 7. We hold the  
8 opinion that it is convenient to adopt a definition of a microtube (or microchannel) as one in which the  
9 diameter (or hydraulic diameter) less than 1000  $\mu\text{m}$ , which is supported by references.<sup>82-86</sup> For the  
10 tested tube with the greatest diameter 1011  $\mu\text{m}$  (which belongs to conventional scale based on the  
11 definition), the critical Reynolds number value is 2009, which fits well with the critical Reynolds  
12 number value (2000) for conventional sized tube<sup>18,26,27,29,30,35,59</sup> within the uncertainty (2%) and also  
13 verifies the validity of this work. For the tested microtube with 776  $\mu\text{m}$  diameter, the critical Reynolds  
14 number value is 1957 and is a little lower than the value 2000. With the further decrease of microtube  
15 diameters, the values of critical Reynolds number decrease. The critical Reynolds number is in the  
16 range of 302-1957 for microtubes with diameters varying from 44.5-776  $\mu\text{m}$ . It is obvious that early  
17 transition happened in microtubes. This phenomenon of early transition is also observed by other  
18 literature.<sup>13,17,18,30-38</sup>

19 As far as now, there are two viewpoints in literature discussing the factors that may lead to an  
20 early transition. Some researchers<sup>13,17,34,38</sup> concluded that the critical Reynolds number decreased with  
21 decreasing diameter, while some other researchers<sup>35-37</sup> believed that it was the increase of roughness

1 led to lower critical Reynolds number. Kandlikar is one of the most representative researchers that  
 2 considered the critical Reynolds number affected by roughness. They<sup>36,37</sup> proposed equations 12 and  
 3 13 based on their own data to calculate the critical Reynolds number.

$$4 \quad 0 \leq \varepsilon / D_{h,cf} \leq 0.08 \quad \text{Re}_{c,cf} = \text{Re}_0 - \frac{\text{Re}_0 - 800}{0.08} \left( \frac{\varepsilon}{D_{h,cf}} \right) \quad (12)$$

$$5 \quad 0.08 \leq \varepsilon / D_{h,cf} \leq 0.15 \quad \text{Re}_{c,cf} = 800 - 32 \left( \frac{\varepsilon}{D_{h,cf}} - 0.08 \right) \quad (13)$$

6 where  $\text{Re}_{h,cf}$  is critical constricted Reynolds number,  $\varepsilon$  is roughness,  $D_{h,cf}$  is constricted hydraulic  
 7 diameter, and  $\text{Re}_0$  is critical Reynolds number for  $\varepsilon \cdot D_{h,cf}^{-1} = 0$ . The average absolute deviation was  
 8 found to be 13% for the 27 experimental data points.

9 However, though equations 12 and 13 work well for Kandlikar's<sup>36,37</sup> own experimental data,  
 10 Zhou and Yao<sup>87</sup> pointed out that Kandlikar's correlation poorly described other random roughness or  
 11 other types of microchannels in literature. To verify whether Kandlikar's correlation was applicative, a  
 12 careful collection of experimental data, including the related diameter, relative roughness and critical  
 13 Reynolds number, was performed in this work. Though a number of references mentioned critical  
 14 Reynolds number, there were only limited references<sup>13,17,26,29,33,34,38</sup> which gave the specific critical  
 15 Reynolds number according to different dimensions of microtubes (or microchannels). References  
 16 which did not list specific critical Reynolds number according to corresponding dimensions were not  
 17 included in this collection. The specific values of critical Reynolds number together with the relevant  
 18 diameter and relative roughness of references are listed in supporting information Table S21, attached  
 19 with the detailed description on the methods to obtain the data sets. Experimental critical Reynolds  
 20 number in this work and references<sup>17,33,34,38</sup> are shown in Figure 6, compared with Kandlikar's

1 correlation (and Kandlikar's experimental data). As can be observed in Figure 6, the deviation  
2 between Kandlikar's correlation and experimental data sets in this work and references<sup>17,33,34</sup> (over  
3 30%) is quite large. Kandlikar mainly focused on the study of microchannels with large roughness (e.g.  
4 17.0  $\mu\text{m}$ <sup>36</sup> and 23.19  $\mu\text{m}$ <sup>37</sup>) and large relative roughness (e.g. 14%<sup>36</sup> and 28%<sup>37</sup>) while the roughness  
5 and relative roughness of most of microtubes (or microchannels) used in references<sup>13,17,26,29,33,34</sup> and  
6 this work was less than 10  $\mu\text{m}$  and 5.00%. The roughness may have large effect on critical Reynolds  
7 number when it is quite large. However, the effect of roughness might be tiny when the roughness is  
8 less than 5.00% and that might explain the reason why Kandlikar's correlation poorly described other  
9 reference data since Kandlikar's correlation is based on the effect of roughness. As also can be  
10 observed in Figure 6, though the critical Reynolds number decreases with the increase of relative  
11 roughness roughly for microtubes with relative roughness larger than 1.00%, the data of microtubes  
12 with relative roughness less than 1.00% (19 data points of critical Reynolds number, including 13 data  
13 points from this work and 6 data points from references,<sup>13,17,34</sup> ranging from 302-2200), clearly show  
14 that there seems no obvious relationship between relative roughness and critical Reynolds number.  
15 The reason why the critical Reynolds number decreases with the increase of relative roughness  
16 roughly when relative roughness is larger than 1.00% might be that for most situations, microtubes (or  
17 microchannels) with smaller diameters always have higher relative roughnesses.

18         Researchers who held the opinion that early transition is caused by the decrease of diameter have  
19 not came up with a relevant equation describing the relationship between critical Reynolds number  
20 and diameter, the quantitative study on the factor that leads to early transition seems to be in a lack.

21         In our case, for microtubes with diameter less than 1000  $\mu\text{m}$ , the critical Reynolds number

1 decreases when the diameter decreases as shown in Figure 7. The critical Reynolds number values of  
2 microtubes with diameters of 523, 526, and 530  $\mu\text{m}$  ( $\varepsilon D^{-1}$  0.42, 0.40, and 0.02%) are 1496, 1518, and  
3 1544, respectively. The microtubes with roughnesses (relative roughnesses) varying from 0.1-2.2  $\mu\text{m}$   
4 (0.02-0.42%) share similar critical Reynolds number. Similar phenomena were also observed for  $\sim 260$   
5 and  $\sim 121$   $\mu\text{m}$  diameter microtubes. These three data sets clearly stated that for microtubes with  
6 roughness (relative roughness) less than 5.2  $\mu\text{m}$  (4.32%), the effect of roughness on the critical  
7 Reynolds number is tiny and can be ignored. It is the decrease of diameter that leads to earlier  
8 transition for microtubes with roughness (relative roughness) less than 5.2  $\mu\text{m}$  (4.32%).

9 We think that the deviation between experimental critical Reynolds number and conventional  
10 theory (2000) can be described as a function of the deviation between microtube diameter and 1000  
11  $\mu\text{m}$  (which is usually adopted as the critical point separating microscale and conventional scale<sup>82-86</sup>).  
12 Thus, a parameter  $\alpha$  was proposed to describe the characteristic of microtube as follow

$$13 \quad \alpha = \frac{1000 - D}{1000} \quad (14)$$

14 where 1000 represents the diameter that separating microscale and conventional scale in  $\mu\text{m}$ ,  $D$  is the  
15 diameter of tested microtubes in  $\mu\text{m}$ . As can be observed from Figure 7, the experimental critical  
16 Reynolds number decreases slowly with the decrease of microtube diameter when the microtube  
17 diameter is larger than 255  $\mu\text{m}$ , while the experimental critical Reynolds number decreases much  
18 quicker with the decrease of microtube diameter when the microtube diameter is smaller than 140.5  
19  $\mu\text{m}$ . So, the characteristic parameter  $\alpha$  was used to calculate the critical Reynolds number for  
20 microscale in the form of segmented function as follows

$$\begin{aligned}
1 \quad \text{Re}_c &= \begin{cases} 2000, & 1000 \mu\text{m} \leq D & \text{(a)} \\ 2000 - 2000 \times 0.46\alpha, & 188 \mu\text{m} \leq D < 1000 \mu\text{m} & \text{(b)} \\ 2000 - 2000 \times (3.33\alpha - 2.33), & 44.5 \mu\text{m} \leq D < 188 \mu\text{m} & \text{(c)} \end{cases} \quad (15)
\end{aligned}$$

2 where  $\text{Re}_c$  is the critical Reynolds number for microscale,  $D$  is diameter of tested microtubes in  $\mu\text{m}$ ,  
3  $188 \mu\text{m}$  is in the range of  $140.5\text{-}255 \mu\text{m}$  and is determined by equations 15(b) and 15(c).

4 The average absolute deviation (AAD) between the calculated critical Reynolds number ( $\text{Re}_{c,\text{calc}}$ )  
5 which was obtained with equation 15 and experimental critical Reynolds number ( $\text{Re}_c$ ) is defined as

$$6 \quad \text{AAD}(\%) = \frac{\sum_{i=1}^{N_p} |100(\text{Re}_{c,\text{calc}} - \text{Re}_c) / \text{Re}_c|_i}{N_p} \quad (16)$$

7 where  $N_p$  represents the number of data points. The AAD is 1.9% for the 20 experimental data points  
8 in this work, with a max deviation of 8.3%. The new obtained equation 15 is shown in Figure 8(a)  
9 together with the experimental data. The deviation between the experimental critical Reynolds number  
10 and calculated critical Reynolds number which is obtained through equation 15 is shown in Figure  
11 8(b). The new equation 15 is also compared with data points from references (listed in supporting  
12 information Table S21) and shown in Figure 8(a). The new correlations basically agree with the  
13 references.<sup>17,26,29,33,34,38</sup> The overall AAD is 5.6% with a max deviation of 23.0% and the detailed  
14 deviations are shown in Figure 8(b).

15 Since the roughness (relative roughness) of the microtubes used in this work is in the range of  
16  $0.1\text{-}5.2 \mu\text{m}$  (0-4.32%) and the roughness (relative roughness) of the microtubes (or microchannels)  
17 used in references<sup>17,26,29,33,34,38</sup> is in the range of  $0.1\text{-}10 \mu\text{m}$  (0-3.70%), thus, equations 15(b) and 15(c)  
18 are only for microtubes (or microchannels) with their roughness (relative roughness) smaller than or

1 equals  $10\ \mu\text{m}$  (4.32%). Fortunately, most commercial available microtubes (or microchannels) own  
2 roughnesses (relative roughnesses) less than  $10\ \mu\text{m}$  (4.32%). The roughness may play a more  
3 important role when roughness is larger than  $10\ \mu\text{m}$ . More researches and data are needed to obtain  
4 more precise and wide applicable correlations.

### 5 3.4 Transitional flow region

6 The values of Reynolds number where turbulent flow begins for each microtube were obtained  
7 using the same method for calculation of critical Reynolds number and are listed in Table 7. It is seen  
8 that there is no evident effect of diameter on the range of transitional region as references<sup>38,44</sup> stated.  
9 There is also no apparent quantitative relation between roughness and the range of transitional region.  
10 However, it is observed that “smooth” microtubes (SS1011, PEEK530, PEEK260, PEEK140.5, and  
11 FS256, the roughness (relative roughness) of these five microtubes is in the range from  $0.1\text{-}0.2\ \mu\text{m}$   
12 ( $0.02\text{-}0.07\%$ )) tend to enter turbulent region earlier than “rough” microtubes (SS776, SS523, SS526,  
13 SS279, SS255, SS263, and SS261, the roughness (relative roughness) of these microtubes is in the  
14 range from  $1.8\text{-}3.0\ \mu\text{m}$  ( $0.23\text{-}1.15\%$ )).

15 The experimental results of  $f$  vs  $Re$  plots in the transitional flow region (start with  $Re_c$  and end  
16 with  $Re_t$ ) of the tested microtubes (diameter  $\geq 140.5\ \mu\text{m}$ ) are shown in Figure 9. It can be observed  
17 from Figure 9 that the friction factor of “rough” microtubes tends to keep decreasing as the increase of  
18 Reynolds number for a much longer range than “smooth” microtubes. Moreover, it is seen that the  
19 “smooth” microtubes tend to have a “smooth” transition (the friction factor in the transitional region  
20 increases slowly as the Reynolds number increases) and “rough” microtubes tend to have a “rough”  
21 transition (the friction factor in the transitional region increases quickly as the Reynolds number

1 increases), which is consistent with the conclusion in literature.<sup>43</sup> For microtubes SS523, SS526,  
2 SS279, SS255, SS263, and SS261, a strange phenomenon was observed. As the pressure increases, the  
3 Reynolds number increases under normal circumstances. However, at one certain location, the  
4 Reynolds number decreases and the friction factor jumps to a much larger value. This phenomenon is  
5 only observed in microtubes with roughness (relative roughness) larger than 2.1 μm (0.40%) and is  
6 thought to be caused by roughness.

### 7 3.5 Turbulent flow region

8 The liquid flow characteristics in turbulent flow are complex even for conventional sized tubes.  
9 Researchers<sup>88-92</sup> are still working on proposing theoretical equation to calculate friction factor in  
10 turbulent flow region. People usually use empirical formulas to describe the relationship between  
11 friction factor and Reynolds number. The most accurate and accepted formulas are Prandtl's formula  
12 (equation 17) for smooth pipes, von Karman's formula (equation 18) for the fully rough regime, and  
13 Colebrook and White's universal formula (equation 19).<sup>93</sup>

$$14 \quad \frac{1}{f^{0.5}} = 2 \log \left( \frac{\text{Re } f^{0.5}}{2.51} \right) \quad (17)$$

$$15 \quad \frac{1}{f^{0.5}} = 2 \log \left( \frac{3.7D}{\varepsilon} \right) \quad (18)$$

$$16 \quad \frac{1}{f^{0.5}} = -2 \log \left( \frac{2.51}{\text{Re } f^{0.5}} + \frac{\varepsilon}{3.7D} \right) \quad (19)$$

17 Equation 19 contains both equations 17 and 18 as limiting cases. However, equations 17 and 19 are  
18 implicit equations which need to be solved by iteration and is inconvenient. Many explicit equations  
19 have been proposed in the literature. Blasius equation (equation 20) and Moody equation (equation 21)

1 which are the most simple and classic formulas are chosen to represent the  $f$  vs Re relationship of  
2 smooth and “rough” (relative roughness in the range of 0-5.00%) conventional sized tubes in this  
3 work.

$$4 \quad f = \frac{0.316}{\text{Re}^{0.25}} \quad (20)$$

$$5 \quad f = 0.0055 \left[ 1 + \left( 2000 \frac{\varepsilon}{D} + \frac{1000000}{\text{Re}} \right)^{1/3} \right] \quad (21)$$

6 The experimental results of  $f$  vs Re plots in the turbulent flow region of the tested microtubes  
7 (diameter  $\geq 140.5 \mu\text{m}$ ) are shown in Figure 10. Figure 11(a) shows the deviation between the  
8 experimental friction factor ( $f_{\text{exp}}$ ) and the calculated friction factor which is obtained through Blasius  
9 equation ( $f_{\text{Blasius}}$ ). It is observed that the experimental friction factor in the turbulent region of tested  
10 microtubes SS1011, PEEK530, PEEK260, PEEK140.5, and FS256 (234 data points) follows the  
11 prediction of Blasius equation perfectly. The AAD is 1.8% for 234 data points with the maximum  
12 deviation equals 5.0%. The experimental friction factor in the turbulent region of SS776, SS523,  
13 SS526, SS279, SS255, SS263, and SS261 (304 data points) is greater than the prediction of Blasius  
14 equation, with an AAD of 8.4% and a maximum deviation of 19.8% for 304 data points. The  
15 calculated friction factor which is obtained through Moody equation ( $f_{\text{Moody}}$ ) is slightly larger than  
16  $f_{\text{Blasius}}$ . As shown in Figure 11(b), the AAD is 2.8% for SS1011, PEEK530, PEEK260, PEEK140.5,  
17 and FS256 (234 data points) with the maximum deviation equals to 7.8%, and 6.4% for SS776, SS523,  
18 SS526, SS279, SS255, SS263, and SS261 (304 data points) with the maximum deviation equals to  
19 19.4%.

20 It is obvious that Blasius equation can still predict the friction factor for smooth microtubes

1 (SS1011, PEEK530, PEEK260, PEEK140.5, and FS256, the roughness (relative roughness) of these  
2 five microtubes is in the range from 0.1-0.2  $\mu\text{m}$  (0.02-0.07%)). However, for rough microtubes  
3 (SS776, SS523, SS526, SS279, SS255, SS263, and SS261, the roughness (relative roughness) of these  
4 seven microtubes is in the range from 1.8-3.0  $\mu\text{m}$  (0.23-1.15%)), the equations for conventional tubes  
5 do not work well. The friction factor is greater than conventional theory and decreases much slower  
6 than conventional theory as the increase of Reynolds number. Hence, we believe that it is the  
7 enhancement of roughness effect that leads to higher friction factor, the same as also mentioned in  
8 literature.<sup>21,36</sup> Some references<sup>21,26,36,40</sup> also have observed higher friction factor, but quantitative study  
9 of friction factor (in turbulent flow) in microscale is in a lack. In this work, an extension of Moody  
10 equation is proposed to predict the friction factor in microscale. The parameters of the two items in  
11 Moody equation,  $\varepsilon D^{-1}$  and  $\text{Re}$ , are modified with the characteristic parameter  $\alpha$  to better predict the  
12 friction factor of microtubes in turbulent flow region as follows

$$13 \quad f = 0.0055 \left[ 1 + \left( (1 - \alpha) \left( 2000(1 + 70\alpha) \frac{\varepsilon}{D} + \frac{1000000}{\text{Re}} \right) \right)^{1/3} \right] \quad (22)$$

14 The extended Moody equation (equation 22) goes back to Moody equation when  $D$  equals 1000  $\mu\text{m}$  ( $\alpha$   
15 equals 0). The new obtained equation 22 is shown in Figure 10 together with the experimental results  
16 of  $f$  vs  $\text{Re}$  relationship in turbulent flow region. The deviation between the experimental friction factor  
17 ( $f_{\text{exp}}$ ) and the calculated friction factor which is obtained through the extended Moody equation ( $f_{\text{this}}$   
18 work) is shown in Figure 12. The AAD is 2.4% with a max deviation of 7.8%. The calculated friction  
19 factor obtained through the extended Moody equation ( $f_{\text{this work}}$ ) presents a good agreement with the  
20 experimental data ( $f_{\text{exp}}$ ). The results show that the extended Moody equation can predict the friction

1 factor in turbulent flow region (Reynolds number range from 2933-11644) for microtubes with  
2 diameters ranging from 255-776  $\mu\text{m}$  and roughness (relative roughness) in the range of 1.8-3.0  $\mu\text{m}$   
3 (0.23-1.15%) with satisfactory precision. More experiments in microtubes with wide range of  
4 diameters and roughnesses need to be conducted to obtain more applicative correlations.

#### 5 **4 Conclusion**

6 Precise measurements, careful experimental methodology and systematical investigations on  
7 liquid flow characteristics in microtubes were performed in this work, using deionized degassed water  
8 as working fluid. The friction factor and Reynolds number (2502 data points) have been obtained over  
9 a Reynolds number range 29-11644 for 20 tested microtubes in the diameter range 44.5-1011  $\mu\text{m}$ , and  
10 in the roughness (relative roughness) range of 0.1-5.2  $\mu\text{m}$  (0.02-4.32%).

11 The conclusions obtained from this work are as follows. 1) In the laminar flow region, the  
12 experimental values of Poiseuille number of all the 20 tested microtubes agree well with the  
13 conventional theory. There shows no effect of roughness on friction factor (in laminar flow) with  
14 roughness (relative roughness) less than 5.2  $\mu\text{m}$  (4.32%). 2) The critical Reynolds number of the  
15 tested microtubes with diameters smaller than 1000  $\mu\text{m}$  is in the range of 302-1957, which means that  
16 early departure from laminar flow happened for these microtubes. The deviation of critical Reynolds  
17 number from conventional theory is found to be caused by the decrease of diameter for microtubes  
18 with roughness (relative roughness) less than 10  $\mu\text{m}$  (4.32%), considering the data obtained from this  
19 work and references. A parameter  $\alpha$  (equation 14) was proposed to describe the characteristic of  
20 microtube. The characteristic parameter  $\alpha$  was used to calculate the critical Reynolds number and a  
21 new equation (equation 15) was obtained for microscale with an AAD of 1.9%. 3) No apparent

1 quantitative relation between roughness and the range of transitional region was observed as stated in  
2 some early references. Nevertheless, smooth microtubes (roughness (relative roughness) in the range  
3 0.1-0.2  $\mu\text{m}$  (0.02-0.07%)) tend to enter turbulent region earlier than rough microtubes (roughness  
4 (relative roughness) in the range 1.8-3.0  $\mu\text{m}$  (0.23-1.15%)) in general. Moreover, the friction factor in  
5 the transitional region increases slowly as the Reynolds number increases for smooth microtubes,  
6 while the friction factor in the transitional region increases quickly as the Reynolds number increases  
7 for rough microtubes. 4) In the turbulent flow region, the friction factor values of microtubes with  
8 roughness (relative roughness) less than 0.2  $\mu\text{m}$  (0.07%) agree well with the Blasius equation, with an  
9 AAD of 1.8%, while the friction factor values of microtubes with roughness (relative roughness) in  
10 the range 1.8-3.0  $\mu\text{m}$  (0.23-1.15%) are much greater than the predictions of Blasius equation or  
11 Moody equation. An extension of Moody equation (equation 22) was proposed with the characteristic  
12 parameter  $\alpha$  to correlate the data of rough microtubes with satisfactory precision (AAD 2.4%).

### 13 **Acknowledgment**

14 Financial support from the National Natural Science Foundation of People's Republic of China  
15 (project-nos: 21176206 and 21306167) is gratefully acknowledged.

16

### 17 **Notation**

$D$	=	diameter, $\mu\text{m}$
$D_h$	=	hydraulic diameter, $\mu\text{m}$
$D_{h,cf}$	=	constricted hydraulic diameter, $\mu\text{m}$
$D_{in}$	=	inlet diameter, $\mu\text{m}$
$D_{out}$	=	outlet diameter, $\mu\text{m}$
$f$	=	friction factor
$fRe$	=	Poiseuille number
$L$	=	length of microtube, m

$L_{\text{long}}$	=	length of the long microtube, m
$L_{\text{short}}$	=	length of the short microtube, m
$M$	=	mass flow rate, $\text{kg}\cdot\text{s}^{-1}$
$N_p$	=	number of data points
$R_a$	=	average roughness, $\mu\text{m}$
$Re$	=	Reynolds number
$Re_c$	=	critical Reynolds number
$Re_{c,\text{calc}}$	=	calculated critical Reynolds number
$Re_{c,\text{cf}}$	=	critical constricted Reynolds number
$Re_t$	=	Reynolds number where turbulent flow begins
$Re_0$	=	critical Reynolds number for $\varepsilon\cdot D_{h,\text{cf}}^{-1} = 0$
$R_q$	=	root mean square roughness, $\mu\text{m}$
$T$	=	fluid temperature, $^{\circ}\text{C}$
$\alpha$	=	characteristic parameter of microtube
$\Delta P$	=	pressure drop, Pa
$\Delta P_D$	=	pressure losses in hydrodynamic development flow, Pa
$\Delta P_{\text{FD}}$	=	fully developed flow pressure drop, Pa
$\Delta P_{\text{in}}$	=	pressure losses in the inlet, Pa
$\Delta P_{\text{long}}$	=	pressure drop along the long microtube, Pa
$\Delta P_{\text{out}}$	=	pressure losses in the outlet, Pa
$\Delta P_{\text{short}}$	=	pressure drop along the short microtube, Pa
$\varepsilon$	=	roughness, $\mu\text{m}$
$\eta$	=	liquid viscosity, Pa·s
$\rho$	=	liquid density, $\text{kg}\cdot\text{m}^{-3}$
$\Sigma K_L$	=	coefficient to represent additional pressure losses

1

2 **Literature Cited:**

- 3 (1) Zhang J, Wang K, Lin X, Lu Y, Luo G. Intensification of fast exothermic reaction by gas agitation in  
4 a microchemical system. *AIChE J.* 2014; 10-1002.
- 5 (2) Fu T, Ma Y, Funfschilling D, Zhu C, Li HZ. Breakup dynamics of slender bubbles in non-newtonian  
6 fluids in microfluidic flow-focusing devices. *AIChE J.* 2012; 58: 3560-3567.
- 7 (3) Sebastian Cabeza V, Kuhn S, Kulkarni AA, Jensen KF. Size-controlled flow synthesis of gold  
8 nanoparticles using a segmented flow microfluidic platform. *Langmuir.* 2012; 28: 7007-7013.
- 9 (4) Noël T, Kuhn S, Musacchio AJ, Jensen KF, Buchwald SL. Suzuki-Miyaura Cross-Coupling reactions  
10 in flow: multistep synthesis enabled by a microfluidic extraction. *Angew. Chem.* 2011; 123: 6065-6068.
- 11 (5) Zhao C, Miller E, Cooper-White JJ, Middelberg APJ. Effects of fluid-fluid interfacial elasticity on  
12 droplet formation in microfluidic devices. *AIChE J.* 2011; 57: 1669-1677.
- 13 (6) Wang K, Lu Y, Yang L, Luo G. Microdroplet coalescences at microchannel junctions with different  
14 collision angles. *AIChE J.* 2013; 59: 643-649.
- 15 (7) Su Y, Chen G, Yuan Q. Influence of hydrodynamics on liquid mixing during Taylor flow in a  
16 microchannel. *AIChE J.* 2012; 58: 1660-1670.

- 1 (8) Su Y, Zhao Y, Jiao F, Chen G, Yuan Q. The intensification of rapid reactions for multiphase systems  
2 in a microchannel reactor by packing microparticles. *AIChE J.* 2011; 57: 1409-1418.
- 3 (9) Salman BH, Mohammed HA, Munisamy KM, Kherbeet AS. Characteristics of heat transfer and fluid  
4 flow in microtube and microchannel using conventional fluids and nanofluids: A review. *Renewable*  
5 *Sustainable Energy Rev.* 2013; 28: 848-880.
- 6 (10) Kandlikar SG. History, advances, and challenges in liquid flow and flow boiling heat transfer in  
7 microchannels: a critical review. *J. Heat Transfer.* 2012; 134: 34001.
- 8 (11) Dey R, Das T, Chakraborty S. Frictional and heat transfer characteristics of single-phase microchannel  
9 liquid flows. *Heat Transfer Eng.* 2011; 33: 425-446.
- 10 (12) Kumar V, Paraschivoiu M, Nigam K. Single-phase fluid flow and mixing in microchannels. *Chem.*  
11 *Eng. Sci.* 2011; 66: 1329-1373.
- 12 (13) Peng XF, Peterson GP, Wang BX. Frictional flow characteristics of water flowing through rectangular  
13 microchannels. *Exp. Heat Transfer.* 1994; 7: 249-264.
- 14 (14) Jiang XN, Zhou ZY, Huang XY, Liu CY. Laminar flow through microchannels used for microscale  
15 cooling systems. *Electron. Packaging Technol. Conf., 1st.* 1997: 119-122.
- 16 (15) Mala GM, Li DQ. Flow characteristics of water in microtubes. *Int. J. Heat Fluid Flow.* 1999; 20:  
17 142-148.
- 18 (16) Stanley RS, Ameen TA, Barron RF *Two-phase flow in microchannels*; DTIC Document: 1997.
- 19 (17) Pfund D, Rector D, Shekarriz A, Popescu A, Welty J. Pressure drop measurements in a microchannel.  
20 *AIChE J.* 2000; 46: 1496-1507.
- 21 (18) Li ZX, Du DX, Guo ZY. Experimental study on flow characteristics of liquid in circular microtubes.  
22 *Microscale Thermophys. Eng.* 2003; 7: 253-265.
- 23 (19) Ergu OB, Sara ON, Yapici S, Arzutug ME. Pressure drop and point mass transfer in a rectangular  
24 microchannel. *Int. Commun. Heat Mass Transfer.* 2009; 36: 618-623.
- 25 (20) Hao PF, He F, Zhu KQ. Flow characteristics in a trapezoidal silicon microchannel. *J. Micromech.*  
26 *Microeng.* 2005; 15: 1362-1368.
- 27 (21) Hrnjak P, Tu X. Single phase pressure drop in microchannels. *Int. J. Heat Fluid Flow.* 2007; 28: 2-14.
- 28 (22) Park HS, Punch J. Friction factor and heat transfer in multiple microchannels with uniform flow  
29 distribution. *Int. J. Heat Mass Transfer.* 2008; 51: 4535-4543.
- 30 (23) Schilder B, Man S, Kasagi N, Hardt S, Stephan P. Flow visualization and local measurement of forced  
31 convection heat transfer in a microtube. *J. Heat Transfer.* 2010; 132: 31702.
- 32 (24) Aniskin VM, Adamenko KV, Maslov AA. Experimental determination of the friction factor  
33 coefficient in microchannels. *J. Appl. Mech. Tech. Phys.* 2011; 52: 18-23.
- 34 (25) Barlak S, Yapici S, Sara ON. Experimental investigation of pressure drop and friction factor for water  
35 flow in microtubes. *Int. J. Therm. Sci.* 2011; 50: 361-368.
- 36 (26) Agostini B, Watel B, Bontemps A, Thonon B. Liquid flow friction factor and heat transfer coefficient  
37 in small channels: an experimental investigation. *Exp. Therm. Fluid Sci.* 2004; 28: 97-103.
- 38 (27) Rands C, Webb BW, Maynes D. Characterization of transition to turbulence in microchannels. *Int. J.*  
39 *Heat Mass Transfer.* 2006; 49: 2924-2930.
- 40 (28) Yang CY, Lin TY. Heat transfer characteristics of water flow in microtubes. *Exp. Therm. Fluid Sci.*  
41 2007; 32: 432-439.

- 1 (29) Dutkowski K. Experimental investigations of Poiseuille number laminar flow of water and air in  
2 minichannels. *Int. J. Heat Mass Transfer*. 2008; 51: 5983-5990.
- 3 (30) Hao PF, Zhang XW, Yao ZH, He F. Transitional and turbulent flow in a circular microtube. *Exp.*  
4 *Therm. Fluid Sci.* 2007; 32: 423-431.
- 5 (31) Xu B, Ooi KT, Wong NT, Choi WK. Experimental investigation of flow friction for liquid flow in  
6 microchannels. *Int. Commun. Heat Mass Transfer*. 2000; 27: 1165-1176.
- 7 (32) Sharp KV, Adrian RJ. Transition from laminar to turbulent flow in liquid filled microtubes. *Exp.*  
8 *Fluids*. 2004; 36: 741-747.
- 9 (33) Liu Z, Zhang C, Huo Y, Zhao X. Flow and heat transfer in rough micro steel tubes. *Exp. Heat*  
10 *Transfer*. 2007; 20: 289-306.
- 11 (34) Zhao Y, Liu Z. Experimental studies on flow visualization and heat transfer characteristics in  
12 microtubes. *Proc. Int. Heat Transfer Conf., 13rd*. 2006.
- 13 (35) Tang GH, Li Z, He YL, Zhao CY, Tao WQ. Experimental observations and lattice Boltzmann method  
14 study of the electroviscous effect for liquid flow in microchannels. *J. Micromech. Microeng.* 2007; 17:  
15 539-550.
- 16 (36) Kandlikar SG, Schmitt D, Carrano AL, Taylor JB. Characterization of surface roughness effects on  
17 pressure drop in single-phase flow in minichannels. *Phys. Fluids*. 2005; 17: 100606.
- 18 (37) Brackbill TP, Kandlikar SG. Effects of low uniform relative roughness on single-phase friction factors  
19 in microchannels and minichannels. *Int. Conf. Nanochannels, Microchannels Minichannels, 5th*. 2007:  
20 509-518.
- 21 (38) Ghajar AJ, Tang CC, Cook WL. Experimental investigation of friction factor in the transition region  
22 for water flow in minitubes and microtubes. *Heat Transfer Eng.* 2010; 31: 646-657.
- 23 (39) Hegab HE, Bari A, Ameel T. Friction and convection studies of R-134a in microchannels within the  
24 transition and turbulent flow regimes. *Exp. Heat Transfer*. 2002; 15: 245-259.
- 25 (40) Celata GP, Cumo M, Guglielmi M, Zummo G. Experimental investigation of hydraulic and  
26 single-phase heat transfer in 0.130-mm capillary tube. *Microscale Thermophys. Eng.* 2002; 6: 85-97.
- 27 (41) Vijayalakshmi K, Anoop KB, Patel HE, Harikrishna PV, Sundararajan T, Das SK. Effects of  
28 compressibility and transition to turbulence on flow through microchannels. *Int. J. Heat Mass Transfer*.  
29 2009; 52: 2196-2204.
- 30 (42) Elsnab JR, Maynes D, Klewicki JC, Ameel TA. Mean flow structure in high aspect ratio microchannel  
31 flows. *Exp. Therm. Fluid Sci.* 2010; 34: 1077-1088.
- 32 (43) Bucci A, Celata GP, Cumo M, Serra E, Zummo G. Water single-phase fluid flow and heat transfer in  
33 capillary tubes. *Int. Conf. Microchannels Minichannels, 1st*. 2003: 319-326.
- 34 (44) Yang CY, Wu JC, Chien HT, Lu SR. Friction characteristics of water, R-134a, and air in small tubes.  
35 *Microscale Thermophys. Eng.* 2003; 7: 335-348.
- 36 (45) Bhatti MS, Shah RK. Laminar convective heat transfer in ducts. In *Handbook of single-phase*  
37 *convective heat transfer*, New York: John Wiley; 1987.
- 38 (46) Colebrook F. Turbulent flow in pipes with particular reference to the transition region between the  
39 smooth and rough pipe laws. *J. Inst. Civ. Eng.* 1939; 11: 133-156.
- 40 (47) Blasius H. Das Ähnlichkeitsgesetz bei Reibungsvorgängen in Flüssigkeiten. *VDI Mitt. Forschungsarb.*  
41 1913; 131 (in German).

- 1 (48) Miller RW. *Flow measurement engineering handbook*. 3rd edition. New York: McGraw-Hill; 1996.
- 2 (49) Churchill SW. Friction factor equations spans all fluid-flow regimes. *Chem. Eng.* 1977; 45: 91-92.
- 3 (50) Ferguson AD, Bahrami M, Culham JR. Review of experimental procedure for determining liquid flow  
4 in microchannels. *Int. Conf. Microchannels Minichannels, 3st.* 2005: 303-311.
- 5 (51) Tang GH, Lu YB, Zhang SX, Wang FF, Tao WQ. Experimental investigation of non-Newtonian  
6 liquid flow in microchannels. *J. Non-Newtonian Fluid Mech.* 2012; 173: 21-29.
- 7 (52) Sara ON, Ergu OB, Arzutug ME, Yapici S. Experimental study of laminar forced convective mass  
8 transfer and pressure drop in microtubes. *Int. J. Therm. Sci.* 2009; 48: 1894-1900.
- 9 (53) Jung JY, Kwak HY. Fluid flow and heat transfer in microchannels with rectangular cross section.  
10 *Heat Mass Transfer.* 2008; 44: 1041-1049.
- 11 (54) Wu K, Zhao C, Xu G, He C. Investigation of convective heat transfer with liquids in microtubes. *Ind.*  
12 *Eng. Chem. Res.* 2012; 51: 9386-9395.
- 13 (55) Hsieh SS, Lin CY, Huang CF, Tsai HH. Liquid flow in a micro-channel. *J. Micromech. Microeng.*  
14 2004; 14: 436-445.
- 15 (56) Peng XF, Peterson GP. Convective heat transfer and flow friction for water flow in microchannel  
16 structures. *Int. J. Heat Mass Transfer.* 1996; 39: 2599-2608.
- 17 (57) Li Z, He YL, Tang GH, Tao WQ. Experimental and numerical studies of liquid flow and heat transfer  
18 in microtubes. *Int. J. Heat Mass Transfer.* 2007; 50: 3447-3460.
- 19 (58) Qu WL, Mala GM, Li DQ. Pressure-driven water flows in trapezoidal silicon microchannels. *Int. J.*  
20 *Heat Mass Transfer.* 2000; 43: 353-364.
- 21 (59) Judy J, Maynes D, Webb BW. Characterization of frictional pressure drop for liquid flows through  
22 microchannels. *Int. J. Heat Mass Transfer.* 2002; 45: 3477-3489.
- 23 (60) Parlak N, Gur M, Ari V, Kucuk H, Engin T. Second law analysis of water flow through smooth  
24 microtubes under adiabatic conditions. *Exp. Therm. Fluid Sci.* 2011; 35: 60-67.
- 25 (61) Shen S, Xu JL, Zhou JJ, Chen Y. Flow and heat transfer in microchannels with rough wall surface.  
26 *Energy Convers. Manage.* 2006; 47: 1311-1325.
- 27 (62) Reynaud S, Debray F, Franc JP, Maitre T. Hydrodynamics and heat transfer in two-dimensional  
28 minichannels. *Int. J. Heat Mass Transfer.* 2005; 48: 3197-3211.
- 29 (63) Brutin D, Topin F, Tadrist L. Transient method for the liquid laminar flow friction factor in  
30 microtubes. *AIChE J.* 2003; 49: 2759-2767.
- 31 (64) Celata GP, Cumo M, McPhail S, Zummo G. Characterization of fluid dynamic behaviour and channel  
32 wall effects in microtube. *Int. J. Heat Fluid Flow.* 2006; 27: 135-143.
- 33 (65) Celata GP, Morini GL, Marconi V, McPhail SJ, Zummo G. Using viscous heating to determine the  
34 friction factor in microchannels--an experimental validation. *Exp. Therm. Fluid Sci.* 2006; 30: 725-731.
- 35 (66) Baviere R, Ayela F, Le Person S, Favre-Marinet M. Experimental characterization of water flow  
36 through smooth rectangular microchannels. *Phys. Fluids.* 2005; 17: 98105.
- 37 (67) Liu D, Garimella SV. Investigation of liquid flow in microchannels. *J. Thermophys. Heat Transfer.*  
38 2004; 18: 65-72.
- 39 (68) Krishnamoorthy C, Ghajar AJ. Single-phase friction factor in micro-tubes: A critical review of  
40 measurement, instrumentation and data reduction techniques from 1991-2006. *Int. Conf. Nanochannels,*  
41 *Microchannels Minichannels, 5th.* 2007: 813-825.

- 1 (69) Lin Z. Study on the flow characteristics of ionic liquid aqueous solution in microtube. M.S. Thesis,  
2 Zhejiang University, P.R.China, 2013.
- 3 (70) Zhou Y. Estimation of physical properties of ionic liquids and study on the flow characteristics of  
4 ionic liquid ethanol solutions in microtubes. M.S. Thesis, Zhejiang University, P.R.China, 2013.
- 5 (71) Kandlikar SG, Joshi S, Tian SR. Effect of surface roughness on heat transfer and fluid flow  
6 characteristics at low reynolds numbers in small diameter tubes. *Heat Transfer Eng.* 2003; 24: 4-16.
- 7 (72) Tu X, Hrnjak P. Experimental investigation of single-phase flow pressure drop through rectangular  
8 microchannels. *Int. Conf. Microchannels Minichannels, 1st.* 2003: 257-267.
- 9 (73) Kohl MJ, Abdel-Khalik SI, Jeter SM, Sadowski DL. An experimental investigation of microchannel  
10 flow with internal pressure measurements. *Int. J. Heat Mass Transfer.* 2005; 48: 1518-1533.
- 11 (74) Cui HH, Silber-Li ZH, Zhu SN. Flow characteristics of liquids in microtubes driven by a high  
12 pressure. *Phys. Fluids.* 2004; 16: 1803-1810.
- 13 (75) Brutin D, Tadrist L. Experimental friction factor of a liquid flow in microtubes. *Phys. Fluids.* 2003; 15:  
14 653-661.
- 15 (76) Zhang XL, Coupland P, Fletcher P, Haswell SJ. Monitoring of liquid flow through microtubes using a  
16 micropressure sensor. *Chem. Eng. Res. Des.* 2009; 87: 19-24.
- 17 (77) Steinke ME, Kandlikar SG. Single-phase liquid friction factors in microchannels. *Int. J. Therm. Sci.*  
18 2006; 45: 1073-1083.
- 19 (78) Streeter VL, Wylie EB. *Fluid mechanics.* 8th edition. New York: McGraw-Hill; 1985.
- 20 (79) Moffat RJ. Describing the uncertainties in experimental results. *Exp. Therm. Fluid Sci.* 1988; 1: 3-17.
- 21 (80) Draad AA, Kuiken GDC, Nieuwstadt FTM. Laminar-turbulent transition in pipe flow for Newtonian  
22 and non-Newtonian fluids. *J. Fluid Mech.* 1998; 377: 267-312.
- 23 (81) Eckhardt B, Schneider TM, Hof B, Westerweel J. Turbulence Transition in Pipe Flow. *Annu. Rev.*  
24 *Fluid Mech.* 2006; 39: 447-468.
- 25 (82) Morini GL. Single-phase convective heat transfer in microchannels: a review of experimental results.  
26 *Int. J. Therm. Sci.* 2004; 43: 631-651.
- 27 (83) Whitesides GM. The origins and the future of microfluidics. *Nature.* 2006; 442: 368-373.
- 28 (84) Hetsroni G, Mosyak A, Pogrebnyak E, Yarin LP. Fluid flow in micro-channels. *Int. J. Heat Mass*  
29 *Transfer.* 2005; 48: 1982-1998.
- 30 (85) Herwig H, Hausner O. Critical view on “new results in micro-fluid mechanics” : an example. *Int. J.*  
31 *Heat Mass Transfer.* 2003; 46: 935-937.
- 32 (86) Obot NT. Toward a better understanding of friction and heat/mass transfer in microchannels-a  
33 literature review. *Microscale Thermophys. Eng.* 2002; 6: 155-173.
- 34 (87) Zhou G, Yao S. Effect of surface roughness on laminar liquid flow in micro-channels. *Appl. Therm.*  
35 *Eng.* 2011; 31: 228-234.
- 36 (88) Barenblatt GI. Scaling laws for fully developed turbulent shear flows. Part I. Basic hypotheses and  
37 analysis. *J. Fluid Mech.* 1993; 248: 513-520.
- 38 (89) Zagarola MV, Smits AJ. Mean-flow scaling of turbulent pipe flow. *J. Fluid Mech.* 1998; 373: 33-79.
- 39 (90) McKeon BJ, Zagarola MV, Smits AJ. A new friction factor relationship for fully developed pipe flow.  
40 *J. Fluid Mech.* 2005; 538: 429-443.
- 41 (91) Shockling MA, Allen JJ, Smits AJ. Roughness effects in turbulent pipe flow. *J. Fluid Mech.* 2006;

- 1 564: 267-285.
- 2 (92) Churchill SW. New simplified models and formulations for turbulent flow and convection. *AIChE J.*
- 3 1997; 43: 1125-1140.
- 4 (93) Haaland SE. Simple and explicit formulas for the friction factor in turbulent pipe flow. *J. Fluids Eng.*
- 5 1983; 105: 89-90.
- 6

1 Caption

2 Table 1 Details about Literature on Liquid Flow Friction Factor (of Laminar Flow) in Microscale

3

4 Table 2 Details about Literature on Liquid Flow Critical Reynolds Number in Microscale

5

6 Table 3 Details about Literature on Liquid Flow Characteristics (of Transitional Flow) in Microscale

7

8 Table 4 Details about Literature on Liquid Flow Friction Factor (of Turbulent Flow) in Microscale

9

10 Table 5 Dimensions of All the Tested Microtubes

11

12 Table 6 Uncertainty in Measured and Calculated Items

13

14 Table 7 The Detailed Experimental Results Including Ranges of Experimental Reynolds Number  $Re$ ,

15 Ranges of Experimental Friction Factor  $f$ , Average Poiseuille Number  $fRe$  of Laminar Flow, Critical

16 Reynolds Number  $Re_c$ , and Reynolds Number Where Turbulent Flow Begins  $Re_t$

17

18 Figure 1 Schematic diagram of the experimental setup.

19

20 Figure 2 Diameter images of one end of tested microtubes, (a) SS1011, (b) SS523, (c) PEEK530, and

21 (d) PEEK75.3. (SS, PEEK stand for stainless steel and poly-ether-ether-ketone, respectively, the

22 number stands for the diameter of tested microtube)

23

24 Figure 3 Roughness images of one section of tested microtubes (a) SS1011, (b) SS523, (c) PEEK530,

25 and (d) SS120.3. (SS, PEEK stand for stainless steel and poly-ether-ether-ketone, respectively, the

26 number stands for the diameter of tested microtube)

27

28 Figure 4 The experimental results of friction factor ( $f$ ) vs Reynolds number ( $Re$ ) relationship for tested

29 microtubes SS1011, SS523, PEEK140.5, and SS120.3, solid line, Hagen-Poiseuille equation, dash line,

30 Blasius equation, dash dot line, Moody equation. (SS, PEEK stand for stainless steel and

31 poly-ether-ether-ketone, respectively, the number stands for the diameter of tested microtube)

32

33 Figure 5 The experimental results of Poiseuille number ( $fRe$ ) vs Reynolds number ( $Re$ ) relationship in

34 laminar flow region and beginning of transitional region and calculation results of critical Reynolds

35 number for all the 20 tested microtubes. (SS, FS, PEEK stand for stainless steel, fused silica, and

36 poly-ether-ether-ketone, respectively, the number stands for the diameter of tested microtube, No 15

37 and No 17 are the numbers of microtubes listed in Table 5)

38

39 Figure 6 The relationship between critical Reynolds number ( $Re_c$ ) and relative roughness ( $\varepsilon D_h^{-1}$ )

40 based on literature data, ■, Kandlikar,<sup>36,37</sup> ●, Pfund et al.,<sup>17</sup> ▲, Zhao and Liu,<sup>34</sup> ▼, Liu et al.,<sup>33</sup> ◆, Ghajar

41 et al.,<sup>38</sup> and □, experimental data in this work, solid line, Kandlikar's correlation.

1

2 Figure 7 The relationship between critical Reynolds number ( $Re_c$ ) and diameter ( $D$ ), □, SS1011,  
3 SS776, PEEK140.5, PEEK102.5, PEEK75.3, PEEK44.5, ○, SS523, SS526, PEEK530, △, SS279,  
4 SS255, SS263, SS261, PEEK260, FS256, ◇, SS120.3, SS121.8, SS120.7(No 15), SS120.6,  
5 SS120.7(No 17). (SS, FS, PEEK stand for stainless steel, fused silica, and poly-ether-ether-ketone,  
6 respectively, the number stands for the diameter of tested microtube, No 15 and No 17 are the  
7 numbers of microtubes listed in Table 5)

8

9 Figure 8 (a) The relationship between experimental critical Reynolds number ( $Re_c$ ) and diameter ( $D$ ),  
10 solid line, equation 15 and (b) relative deviation between experimental critical Reynolds number ( $Re_c$ )  
11 and calculated critical Reynolds number ( $Re_{c,calc}$ ) which is obtained through equation 15: ■, this work,  
12 ●, Pfund et al.,<sup>17</sup> ▲, Agostini et al.,<sup>26</sup> ▼, Zhao and Liu,<sup>34</sup> ◆, Liu et al.,<sup>33</sup> ★, Dutkowski,<sup>29</sup> +, Ghajar et  
13 al.<sup>38</sup>

14

15 Figure 9 The experimental results of friction factor ( $f$ ) vs Reynolds number ( $Re$ ) relationship in  
16 transitional flow region (start with  $Re_c$  and end with  $Re_t$ ) of the tested microtubes with diameter  $\geq$   
17 140.5  $\mu\text{m}$ , solid line, Hagen-Poiseuille equation. (SS, FS, PEEK stand for stainless steel, fused silica,  
18 and poly-ether-ether-ketone, respectively, the number stands for the diameter of tested microtube)

19

20 Figure 10 The experimental results of friction factor ( $f$ ) vs Reynolds number ( $Re$ ) relationship in  
21 turbulent flow region of the tested microtubes with diameter  $\geq 140.5 \mu\text{m}$ , solid line, Hagen-Poiseuille  
22 equation, dash line, Blasius equation, dash dot line, extended Moody equation (equation 22). (SS, FS,  
23 PEEK stand for stainless steel, fused silica, and poly-ether-ether-ketone, respectively, the number  
24 stands for the diameter of tested microtube)

25

26 Figure 11 The deviation between the experimental friction factor ( $f_{exp}$ ) and (a) the calculated friction  
27 factor which is obtained through Blasius equation ( $f_{Blasius}$ ), (b) the calculated friction factor which is  
28 obtained through Moody equation ( $f_{Moody}$ ) for all the 538 data points in turbulent flow region, ■,  
29 SS1011, ●, PEEK530, ▲, PEEK260, ▼, PEEK140.5, ◆, FS256, □, SS776, ○, SS523, △, SS526, ▽,  
30 SS279, ◇, SS255, ◁, SS263, ▷, SS261. (SS, FS, PEEK stand for stainless steel, fused silica, and  
31 poly-ether-ether-ketone, respectively, the number stands for the diameter of tested microtube)

32

33 Figure 12 The deviation between the experimental friction factor ( $f_{exp}$ ) and the calculated friction  
34 factor which is obtained through the extended Moody equation (equation 22) ( $f_{this\ work}$ ) for the 304 data  
35 points in turbulent flow region of rough microtubes, □, SS776, ○, SS523, △, SS526, ▽, SS279, ◇,  
36 SS255, ◁, SS263, ▷, SS261. (SS, FS, PEEK stand for stainless steel, fused silica, and  
37 poly-ether-ether-ketone, respectively, the number stands for the diameter of tested microtube)

1 Table 1 Details about Literature on Liquid Flow Friction Factor (of Laminar Flow) in Microscale

Reference	Material	Geometry	Test fluids	$D_h$ ( $\mu\text{m}$ )	$\varepsilon D_h^{-1}$ (%)	Re	$(f\text{Re})_{\text{exp}} / (f\text{Re})_{\text{the}}^{-1}$ (laminar flow)	Uncertainty in $f$ (%)
Peng et al. <sup>13</sup>	SS	Rectangle	Water	133-343	0.6-1	50-4000	<1	10
Jiang et al. <sup>14</sup>	Silicon	Trapezoid	Water	35-120	<0.4	1-30	<1	-
Mala et al. <sup>15</sup>	SS,FS	Circular	Water	50-254	0.7-3.5	100-2000	>1	9.2
Stanley et al. <sup>16</sup>	Aluminum	Rectangle	Water	56-256	0-0.16	50-10000	>1	-
Pfund et al. <sup>17</sup>	Polymide	Rectangle	Water	253-1900	Smooth	60-3450	>1	5.4-11.1 (uncertainty in $f\text{Re}$ )
Li et al. <sup>18</sup>	SS	Circular	Water	128.76-179.8	3-4	350-2500	>1	<10 (uncertainty in $f\text{Re}$ )
Ergu et al. <sup>19</sup>	Acrylic	Rectangle	Water	208	Smooth	100-845	>1	18.77
Hao et al. <sup>20</sup>	Silicon	Trapezoid	Water	237	0.025	50-2800	$\approx 1$	-
Hrnjak and Tu <sup>21</sup>	PVC	Rectangle	R134a	69.5-304.7	0.14-0.35	112-9180	$\approx 1$	6.2
Park and Punch <sup>22</sup>	Silicon	Rectangle	Water	106-307	Smooth	69-800	$\approx 1$	9.2
Schilder et al. <sup>23</sup>	Glass	Circular	Water	600	Smooth	20-1200	$\approx 1$	-
Aniskin et al. <sup>24</sup>	Glass	Circular	Water	24.5-34.5	Smooth	13-330	$\approx 1$	-
Barlak et al. <sup>25</sup>	SS	Circular	Water	200-589	-	75-10461	$\approx 1$	12.92-19.76

2 Note: SS, FS stand for stainless steel and fused silica, respectively

1 Table 2 Details about Literature on Liquid Flow Critical Reynolds Number in Microscale

Reference	Material	Geometry	Test fluids	$D_h$ ( $\mu\text{m}$ )	$\varepsilon D_h^{-1}$ (%)	Re	Early $Re_c$	Uncertainty in $f$ (%)
Agostini et al. <sup>26</sup>	Aluminum	Rectangle	R-134a	770-1170	-	500-6500	No	7-15
Rands et al. <sup>27</sup>	FS	Circular	Water	16.6-32.2	0.03-0.04	300-3400	No	16-29 (uncertainty in $fRe$ )
Yang and Lin <sup>28</sup>	SS	Circular	Water	123-962	0.15-1.14	150-10000	No	0.2-5.3
Dutkowski <sup>29</sup>	SS	Circular	Water	550-1100	-	30-6500	No	-
Li et al. <sup>18</sup>	SS	Circular	Water	128.76	3-4	350-2500	Yes	<10 (uncertainty in $fRe$ )
Hao et al. <sup>30</sup>	Glass	Circular	Water	230	0.74	1540-2960	Yes	-
Xu et al. <sup>31</sup>	Silicon	Rectangle	Water	30-344	<1	20-4000	Yes	<12
Sharp and Adrian <sup>32</sup>	Glass	Circular	Water	50-247	-	20-2900	Yes	-
Liu et al. <sup>33</sup>	SS	Circular	Water	168-399	2.7-3.5	100-3000	Yes	7.5
Peng et al. <sup>13</sup>	SS	Rectangle	Water	133-343	0.6-1	50-4000	Yes	10
Pfund et al. <sup>17</sup>	Polymide	Rectangle	Water	253-1900	Smooth	60-3450	Yes	5.4-11.1 (uncertainty in $fRe$ )
Zhao and Liu <sup>34</sup>	SS,FS	Circular	Water	168-799	0-8	50-2700	Yes	6.5
Tang et al. <sup>35</sup>	SS	Circular	Water	119-172	4.1-5.9	10.5-1100	Yes	6.3
Kandlikar et al. <sup>36</sup>	-	Rectangle	Water	325-1819	0-14	200-5700	Yes	8.81
Brackbill and Kandlikar <sup>37</sup>	-	Rectangle	Water	198-1084	0-5.18	30-7000	Yes	7.58
Ghajar et al. <sup>38</sup>	SS	Circular	Water	337-2083	1-4	500-7000	Yes	-

2 Note: SS, FS stand for stainless steel and fused silica, respectively

1 Table 3 Details about Literature on Liquid Flow Characteristics (of Transitional Flow) in Microscale

Reference	Material	Geometry	Test fluids	$D_h$ ( $\mu\text{m}$ )	$\varepsilon D_h^{-1}$ (%)	Re	Transitional Flow Characteristics	Uncertainty in $f$ (%)
Hegab et al. <sup>39</sup>	Aluminum	Rectangle	R-134a	112-210	0.16-0.89	1280-13000	$Re_t$ 4000	3-23
Celata et al. <sup>40</sup>	SS	Circular	R114	130	2.65	100-8000	$Re_t$ 2480	6-9
Yang and Lin <sup>28</sup>	SS	Circular	Water	123-962	0.15-1.14	150-10000	$Re_t$ 3000	0.2-5.3
Hao et al. <sup>30</sup>	Glass	Circular	Water	230	0.74	1540-2960	$Re_t$ 2500	-
Vijayalakshmi et al. <sup>41</sup>	Silicon	Trapezoid	Water	60.5-211	0.04-0.18	320-2791	$Re_t$ 3500	0.12-5.34
Elsnab et al. <sup>42</sup>	Aluminum	Rectangle	Water	923	0.06	173-4830	$Re_t$ 2700	-
Bucci et al. <sup>43</sup>	SS	Circular	Water	172	0.87	100-3600	rough transition	8.36
Yang et al. <sup>44</sup>	-	Circular	Water, R-134a	502-4010	-	110-40000	increases with decreasing tube diameters	4.1-9.0
Ghajar et al. <sup>38</sup>	SS	Circular	Water	337-667	1-4	500-7000	narrower	-
Barlak et al. <sup>25</sup>	SS	Circular	Water	200-589	-	75-10461	smooth and rough transition	12.92-19.76

2 Note: SS stands for stainless steel

1 Table 4 Details about Literature on Liquid Flow Friction Factor (of Turbulent Flow) in Microscale

Reference	Material	Geometry	Test fluids	$D_h$ ( $\mu\text{m}$ )	$\varepsilon D_h^{-1}$ (%)	Re	$f$ (turbulent flow)	Uncertainty in $f$ (%)
Hegab et al. <sup>39</sup>	Aluminum	Rectangle	R-134a	112-210	0.16-0.89	1280-13000	< Bhati and Shah equation <sup>45</sup>	3-23
Bucci et al. <sup>43</sup>	SS	Circular	Water	290-520	0.31-0.75	100-6000	$\approx$ Colebrook correlation <sup>46</sup>	8.36
Yang et al. <sup>44</sup>	-	Circular	Water, R-134a	502-4010	-	110-40000	$\approx$ Blasius equation <sup>47</sup>	4.1-9.0
Yang and Lin <sup>28</sup>	SS	Circular	Water	123-962	0.15-1.14	150-10000	$\approx$ Blasius equation <sup>47</sup>	0.2-5.3
Celata et al. <sup>40</sup>	SS	Circular	R114	130	2.65	100-8000	Colebrook equation <sup>46</sup> > $f$ > Blasius equation <sup>47</sup>	6-9
Agostini et al. <sup>26</sup>	Aluminum	Rectangle	R-134a	770-1170	-	500-6500	>Blasius equation <sup>47</sup>	7-15
Kandlikar et al. <sup>36</sup>	-	Rectangle	Water	684-953	7.35-11.08	200-3000	>Miller equation <sup>48</sup>	8.81
Hrnjak and Tu <sup>21</sup>	PVC	Rectangle	R-134a	104.1-304.7	0.14-0.35	112-9180	> Churchill equation <sup>49</sup>	4.5-6.3

2 Note: SS stands for stainless steel

3 Bhati and Shah equation:<sup>45</sup>  $f = \frac{0.611}{\text{Re}^{0.35}}$

4 Colebrook equation:<sup>46</sup>  $\frac{1}{f^{0.5}} = 2 \log \left( \frac{2.51}{\text{Re} f^{0.5}} \right) + \frac{\varepsilon}{3.7}$

5 Blasius equation:<sup>47</sup>  $f = \frac{0.316}{\text{Re}^{0.25}}$

6 Miller equation:<sup>48</sup>  $f = 0.25 \left[ \ln \left( \frac{\varepsilon/D_h}{3.7} + \frac{5.74}{\text{Re}^{0.9}} \right) \right]^{-2}$

7 Churchill equation:<sup>49</sup>

8  $f = 8 \left[ \left( \frac{8}{\text{Re}} \right)^{12} + \left( \left[ -2.457 \ln \left( \left( \frac{7}{\text{Re}} \right)^{0.9} + 0.27 \left( \frac{\varepsilon}{D} \right) \right) \right]^{16} + \left( \frac{37530}{\text{Re}} \right)^{16} \right)^{-1.5} \right]^{1/12}$

1 Table 5 Dimensions of All the Tested Microtubes

No.	Material	Length $L$ (mm)	Inlet Diameter $D_{in}$ ( $\mu\text{m}$ )	Outlet Diameter $D_{out}$ ( $\mu\text{m}$ )	Diameter $D$ ( $\mu\text{m}$ )	Roughness $\varepsilon$ ( $\mu\text{m}$ )	Relative Roughness $\varepsilon D^{-1}$ (%)
1	SS	1830	1011	1012	1011	0.2	0.02
2	SS	1000	776	776	776	1.8	0.23
3	SS	500	523	524	523	2.2	0.42
4	SS	500	526	526	526	2.1	0.40
5	PEEK	500	532	529	530	0.1	0.02
6	SS	200.0	280	279	279	2.5	0.90
7	SS	200.0	254	255	255	2.7	1.06
8	SS	200.0	262	263	263	2.6	0.99
9	SS	200.0	261	261	261	3.0	1.15
10	PEEK	200.0	261	260	260	0.1	0.04
11	FS	200.0	257	255	256	0.1 <sup>a</sup>	0.04
12	PEEK	100.0	141.1	139.9	140.5	0.1 <sup>b</sup>	0.07
13	SS	100.0	120.4	120.2	120.3	5.2	4.32
14	SS	100.0	122.0	121.6	121.8	3.3	2.71
15	SS	100.0	120.7	120.7	120.7	3.5	2.90
16	SS	100.0	120.6	120.7	120.6	4.5	3.73
17	SS	100.0	120.4	121.0	120.7	4.0	3.31
18	PEEK	69.5	102.6	102.3	102.5	0.1 <sup>b</sup>	0.10
19	PEEK	40.0	75.4	75.1	75.3	0.1 <sup>b</sup>	0.13
20	PEEK	24.0	43.7	43.3	44.5	0.1 <sup>b</sup>	0.22

2 Note: SS, PEEK, and FS stand for stainless steel, poly-ether-ether-ketone, and fused silica, respectively, <sup>a</sup> the roughness  
3 is decided according to literature values, <sup>b</sup> the roughness is decided according to the measured roughness values of the  
4 same type (PEEK) of microtubes and literature values.

1 Table 6 Uncertainty in Measured and Calculated Items

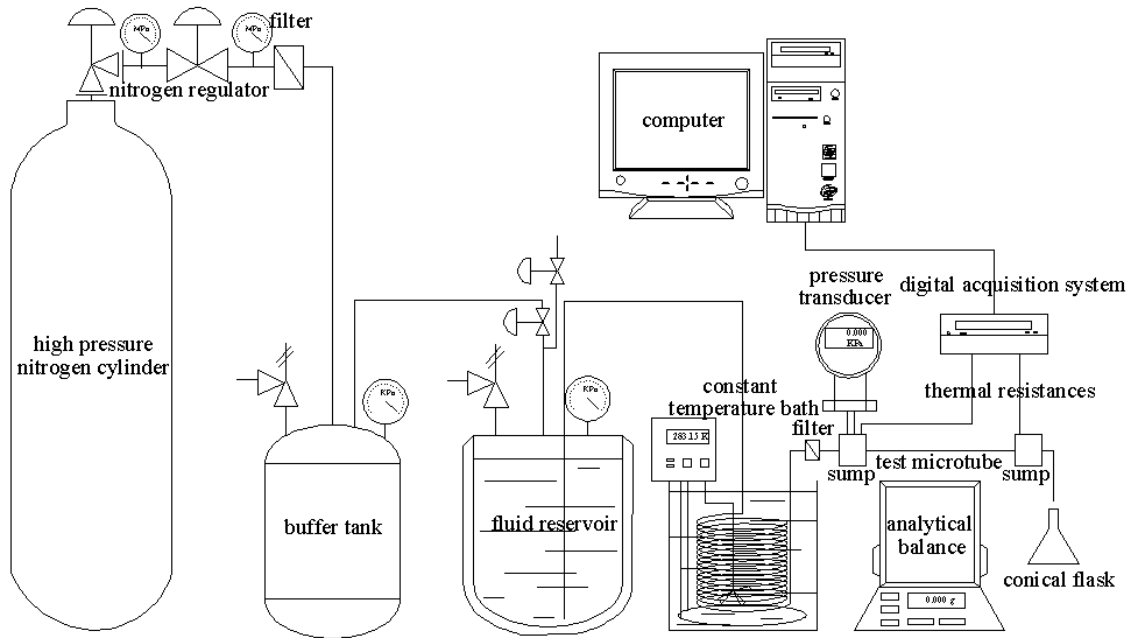
Items	$\delta M/M$	$\delta \eta/\eta$	$\delta D/D$	$\delta \Delta P/\Delta P$	$\delta \rho/\rho$	$\delta L/L$	$\delta Re/Re$	$\delta f/f$	$\delta Re/fRe$
Uncertainty (%)	0.1	1	1	0.075	0.01	0.1	1.42	5.01	4.13

2

1 Table 7 The Detailed Experimental Results Including Ranges of Experimental Reynolds Number  $Re$ ,  
 2 Ranges of Experimental Friction Factor  $f$ , Average Poiseuille Number  $fRe$  of Laminar Flow, Critical  
 3 Reynolds Number  $Re_c$ , and Reynolds Number Where Turbulent Flow Begins  $Re_t$

Tested microtubes	$Re$ range	$f$ range	$(fRe)_{\text{laminar,ave}}$	$Re_c$	$Re_t$
SS1011	903-11101	0.0263-0.0705	64	2009	3113
SS776	1073-11644	0.0265-0.0599	64	1957	2933
SS523	591-8473	0.0217-0.1093	64	1496	4004
SS526	748-8645	0.0192-0.0853	64	1518	4052
PEEK530	404-4759	0.0345-0.1596	64	1544	2553
SS279	303-5452	0.0251-0.2104	64	1321	3340
SS255	169-4534	0.0252-0.3746	63	1336	3200
SS263	167-4646	0.0227-0.3805	63	1331	3455
SS261	237-4611	0.0211-0.2703	64	1315	4048
PEEK260	159-4658	0.0343-0.4013	64	1331	2612
FS256	232-4605	0.0322-0.2770	64	1306	2793
PEEK140.5	93-3793	0.0357-0.5858	64	939	2595
SS120.3	132-2041	0.0355-0.4817	64	817	-
SS121.8	101-2068	0.0358-0.6268	64	849	-
SS120.7(No 15)	142-2007	0.0369-0.4463	64	836	-
SS120.6	129-2033	0.0365-0.4937	64	809	-
SS120.7(No 17)	134-2113	0.0362-0.4761	64	799	-
PEEK102.5	109-2280	0.0354-0.6927	63	680	-
PEEK75.3	44-1973	0.0358-1.4476	64	494	-
PEEK44.5	29-656	0.1024-2.2084	64	302	-

4 Note: SS, FS, PEEK stand for stainless steel, fused silica, and poly-ether-ether-ketone, respectively, the number stands  
 5 for the diameter of tested microtube, No 15 and No 17 are the numbers of microtubes listed in Table 5.

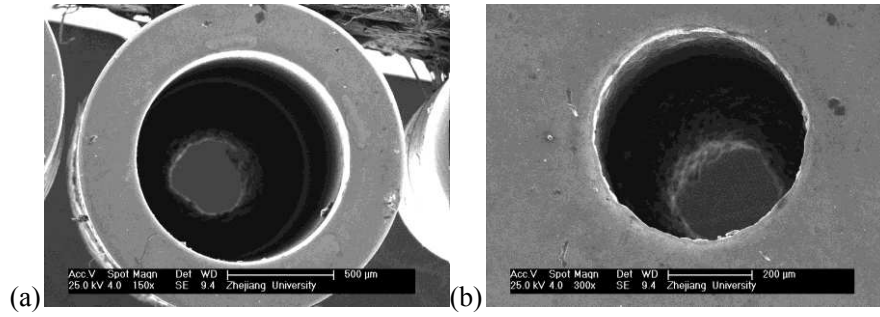


1

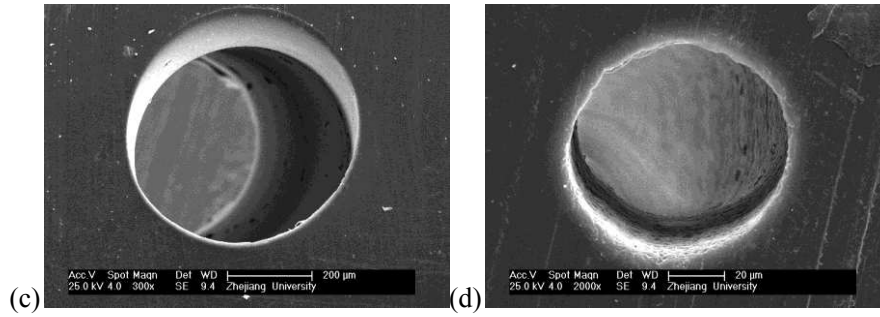
2

Figure 1 Schematic diagram of the experimental setup.

1



2



3 Figure 2 Diameter images of one end of tested microtubes, (a) SS1011, (b) SS523, (c) PEEK530, and  
4 (d) PEEK75.3. (SS, PEEK stand for stainless steel and poly-ether-ether-ketone, respectively, the  
5 number stands for the diameter of tested microtube)

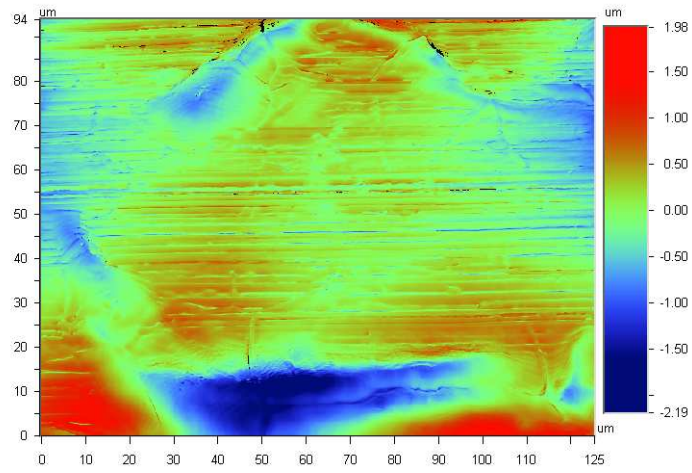
1

(a)

**Surface Statistics:**  
Ra: 355.52 nm  
Rq: 483.43 nm  
Rz: 3.78 um  
Rt: 4.17 um

**Set-up Parameters:**  
Size: 640 X 480  
Sampling: 196.16 nm

**Processed Options:**  
Terms Removed:  
Cylinder & Tilt  
Filtering:  
None



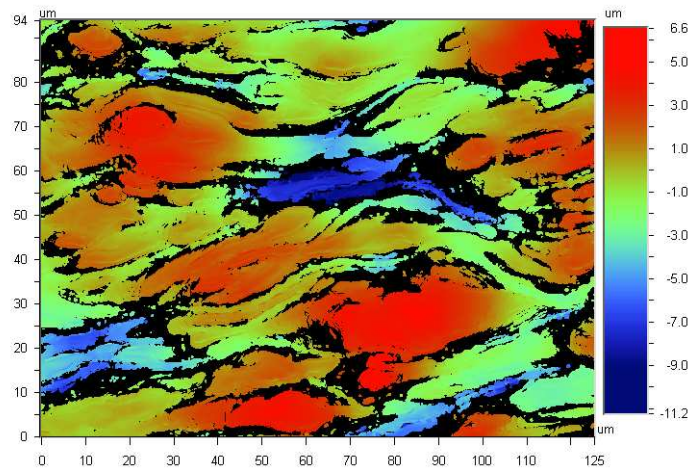
2

(b)

**Surface Statistics:**  
Ra: 1.97 um  
Rq: 2.57 um  
Rz: 16.35 um  
Rt: 17.79 um

**Set-up Parameters:**  
Size: 640 X 480  
Sampling: 196.16 nm

**Processed Options:**  
Terms Removed:  
Cylinder & Tilt  
Filtering:  
None

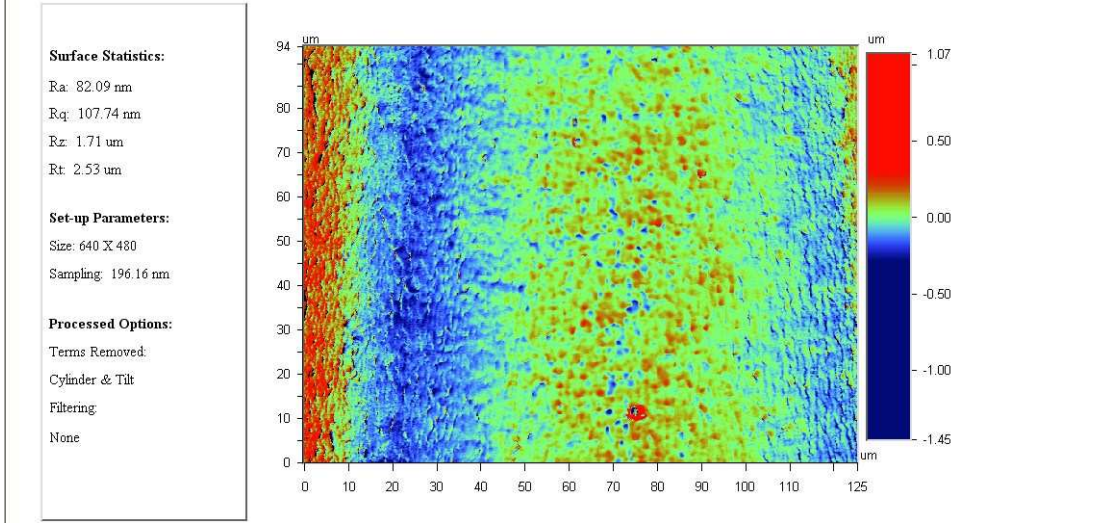


4

(c)

5

1  
2



(d)

3  
4  
5  
6  
7

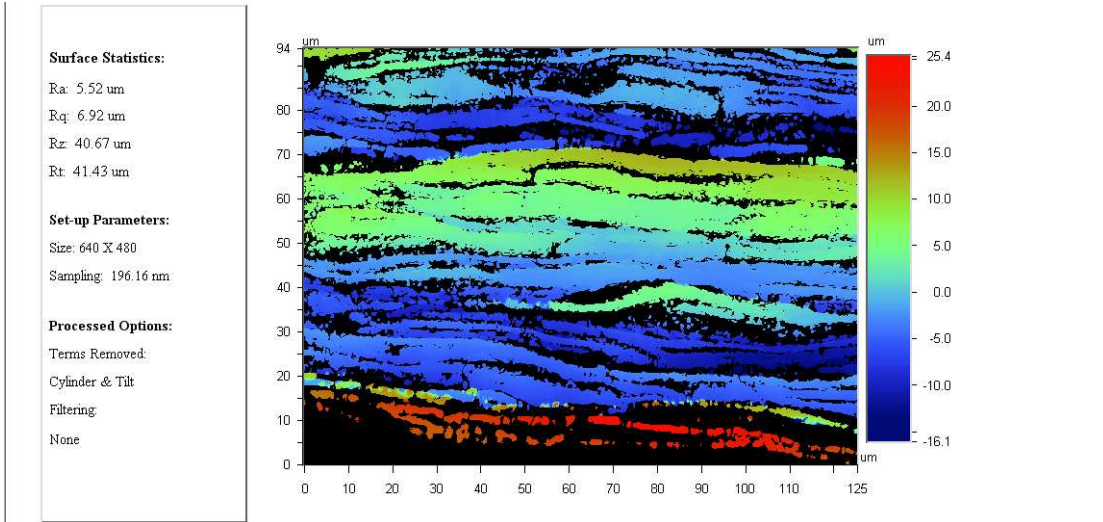
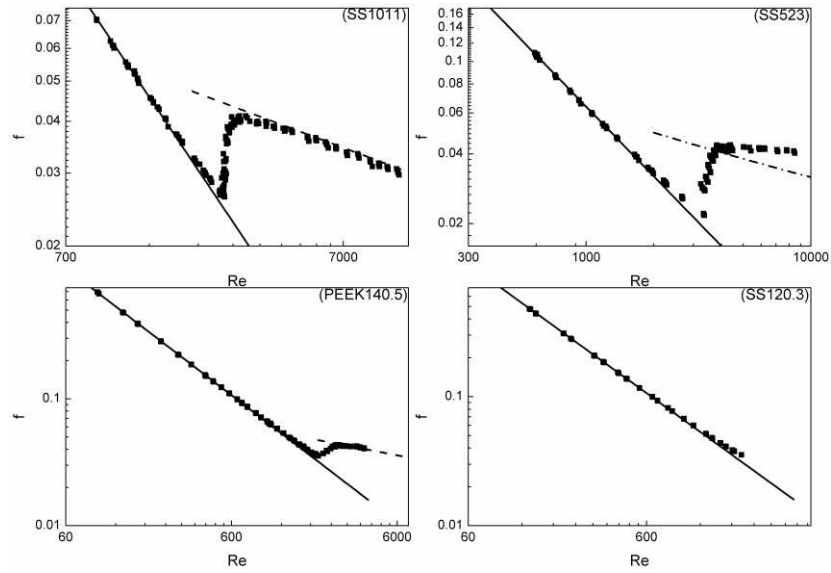
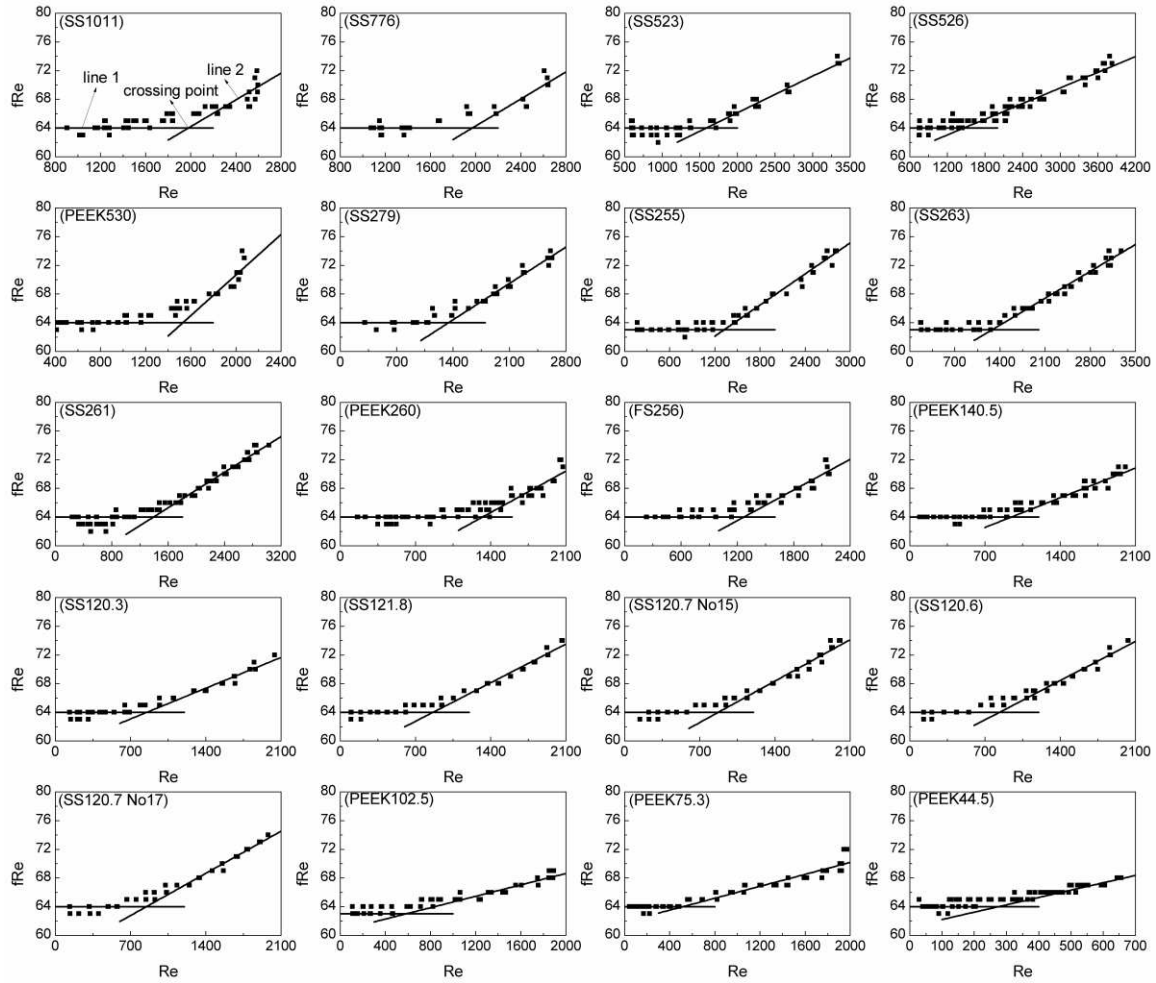


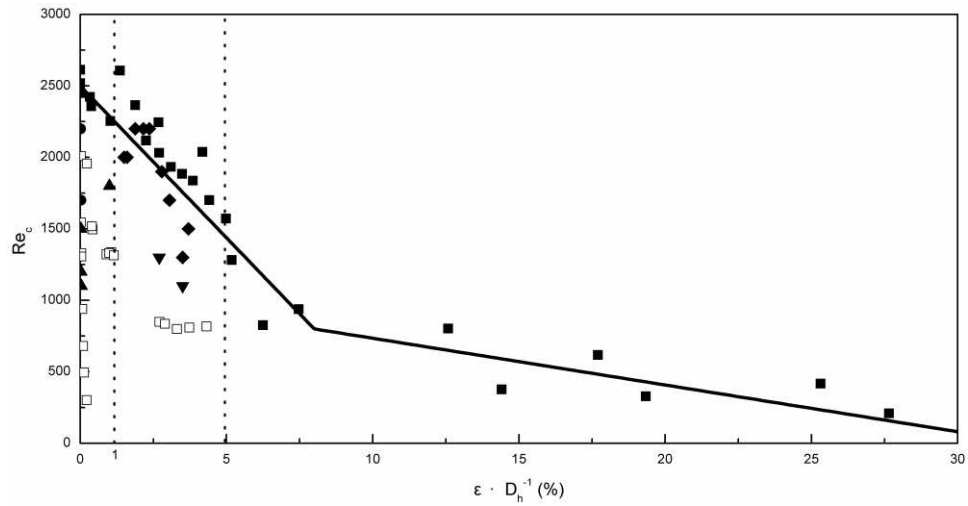
Figure 3 Roughness images of one section of tested microtubes (a) SS1011, (b) SS523, (c) PEEK530, and (d) SS120.3. (SS, PEEK stand for stainless steel and poly-ether-ether-ketone, respectively, the number stands for the diameter of tested microtube)



1  
 2 Figure 4 The experimental results of friction factor ( $f$ ) vs Reynolds number ( $Re$ ) relationship for tested  
 3 microtubes SS1011, SS523, PEEK140.5, and SS120.3, solid line, Hagen-Poiseuille equation, dash line,  
 4 Blasius equation, dash dot line, Moody equation. (SS, PEEK stand for stainless steel and  
 5 poly-ether-ether-ketone, respectively, the number stands for the diameter of tested microtube)

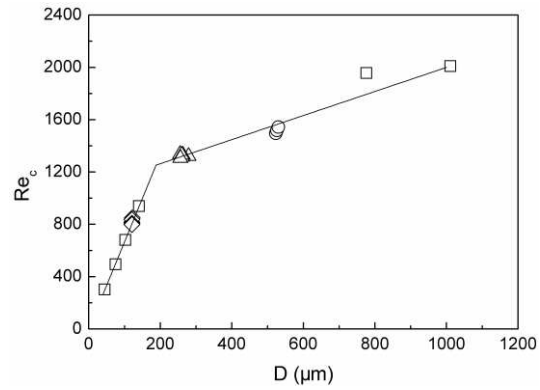


1  
 2 Figure 5 The experimental results of Poiseuille number ( $fRe$ ) vs Reynolds number ( $Re$ ) relationship in  
 3 laminar flow region and beginning of transitional region and calculation results of critical Reynolds  
 4 number for all the 20 tested microtubes. (SS, FS, PEEK stand for stainless steel, fused silica, and  
 5 poly-ether-ether-ketone, respectively, the number stands for the diameter of tested microtube, No 15  
 6 and No 17 are the numbers of microtubes listed in Table 5)



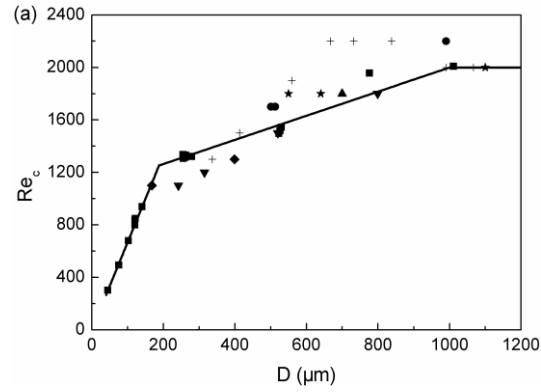
1  
2  
3  
4  
5  
6

Figure 6 The relationship between critical Reynolds number ( $Re_c$ ) and relative roughness ( $\varepsilon \cdot D_h^{-1}$ ) based on literature data, ■, Kandlikar,<sup>36,37</sup> ●, Pfund et al.,<sup>17</sup> ▲, Zhao and Liu,<sup>34</sup> ▼, Liu et al.,<sup>33</sup> ◆, Ghajar et al.,<sup>38</sup> and □, experimental data in this work, solid line, Kandlikar's correlation.

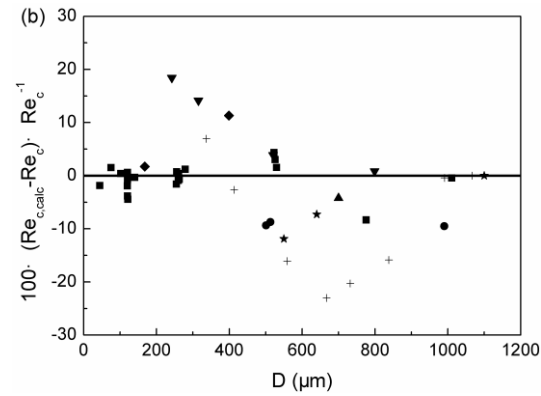


1  
2  
3  
4  
5  
6  
7  
8

Figure 7 The relationship between critical Reynolds number ( $Re_c$ ) and diameter ( $D$ ),  $\square$ , SS1011, SS776, PEEK140.5, PEEK102.5, PEEK75.3, PEEK44.5,  $\circ$ , SS523, SS526, PEEK530,  $\triangle$ , SS279, SS255, SS263, SS261, PEEK260, FS256,  $\diamond$ , SS120.3, SS121.8, SS120.7(No 15), SS120.6, SS120.7(No 17). (SS, FS, PEEK stand for stainless steel, fused silica, and poly-ether-ether-ketone, respectively, the number stands for the diameter of tested microtube, No 15 and No 17 are the numbers of microtubes listed in Table 5)

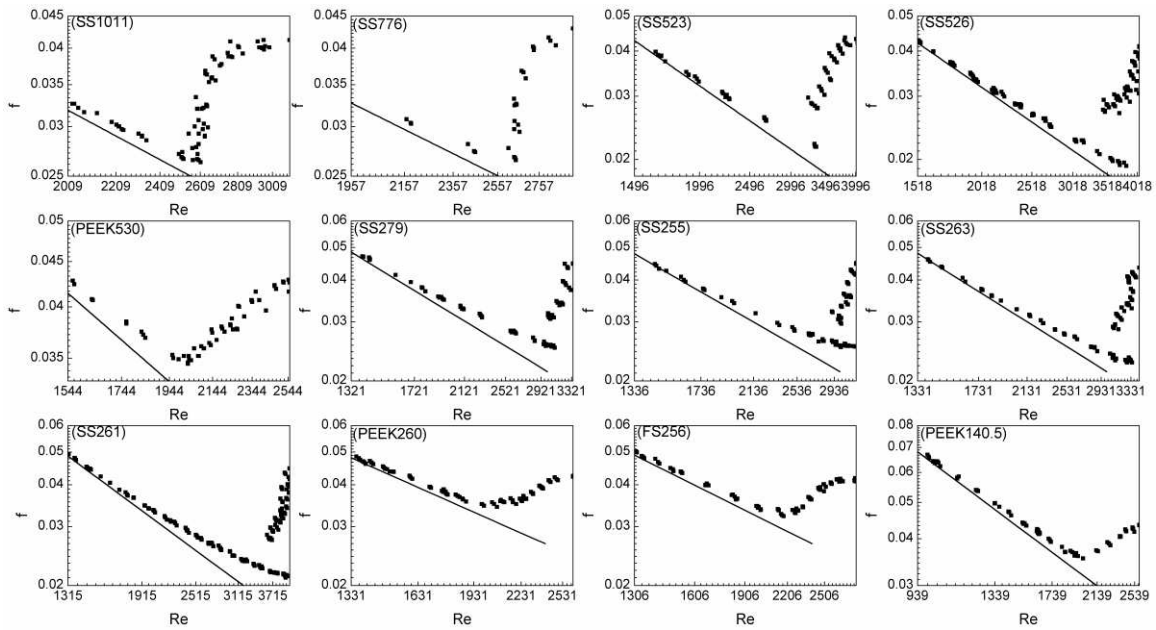


1



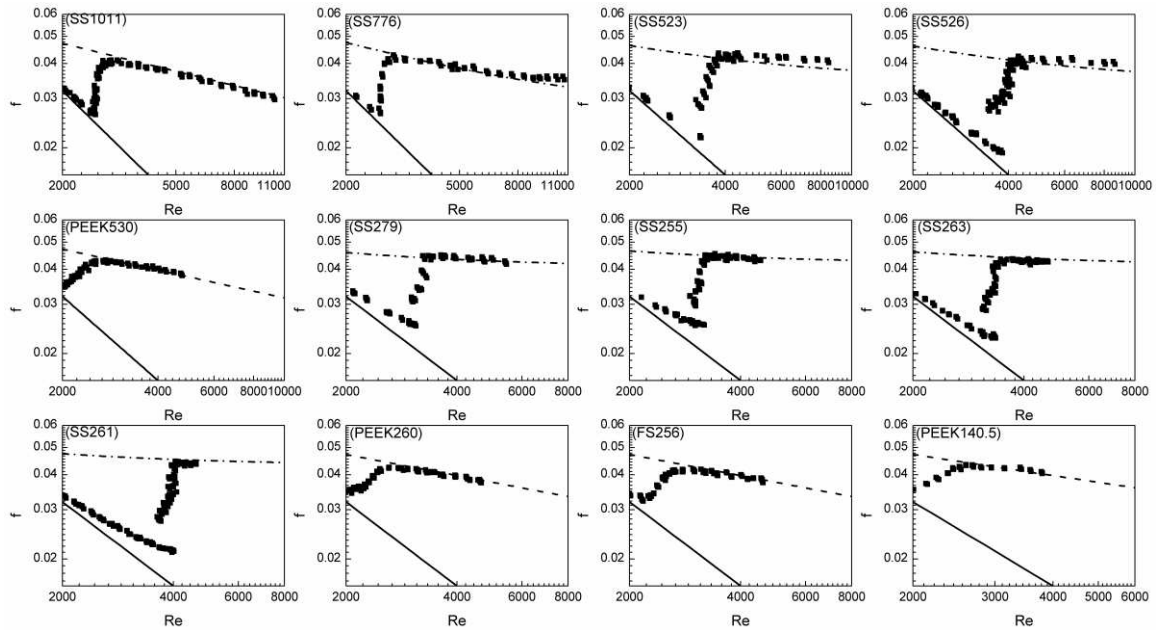
2

3 Figure 8 (a) The relationship between experimental critical Reynolds number ( $Re_c$ ) and diameter ( $D$ ),  
 4 solid line, equation 15 and (b) relative deviation between experimental critical Reynolds number ( $Re_c$ )  
 5 and calculated critical Reynolds number ( $Re_{c,calc}$ ) which is obtained through equation 15: ■, this work,  
 6 ●, Pfund et al.,<sup>17</sup> ▲, Agostini et al.,<sup>26</sup> ▼, Zhao and Liu,<sup>34</sup> ◆, Liu et al.,<sup>33</sup> ★, Dutkowski,<sup>29</sup> +, Ghajar et  
 7 al.<sup>38</sup>



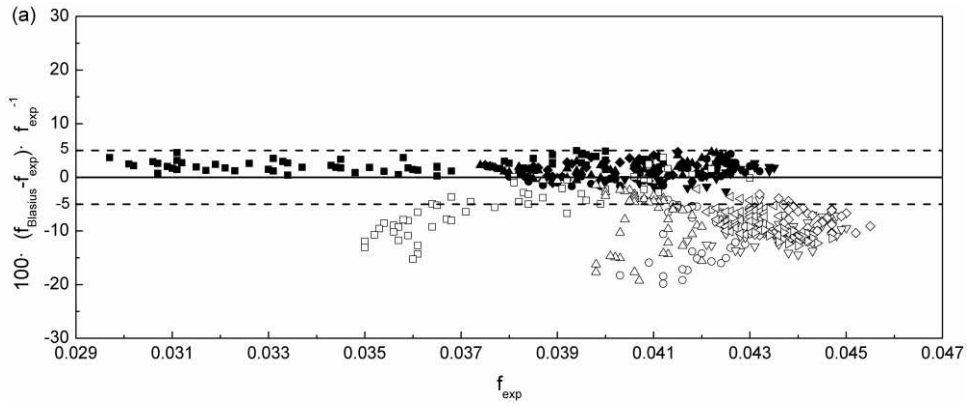
1  
2  
3  
4  
5  
6

Figure 9 The experimental results of friction factor ( $f$ ) vs Reynolds number ( $Re$ ) relationship in transitional flow region (start with  $Re_c$  and end with  $Re_t$ ) of the tested microtubes with diameter  $\geq 140.5 \mu\text{m}$ , solid line, Hagen-Poiseuille equation. (SS, FS, PEEK stand for stainless steel, fused silica, and poly-ether-ether-ketone, respectively, the number stands for the diameter of tested microtube)

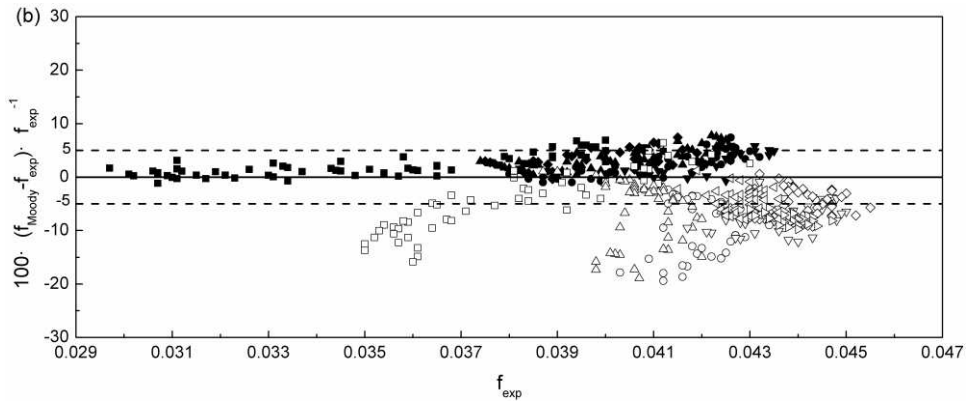


1  
2  
3  
4  
5  
6  
7

Figure 10 The experimental results of friction factor ( $f$ ) vs Reynolds number ( $Re$ ) relationship in turbulent flow region of the tested microtubes with diameter  $\geq 140.5 \mu\text{m}$ , solid line, Hagen-Poiseuille equation, dash line, Blasius equation, dash dot line, extended Moody equation (equation 22). (SS, FS, PEEK stand for stainless steel, fused silica, and poly-ether-ether-ketone, respectively, the number stands for the diameter of tested microtube)



1



2

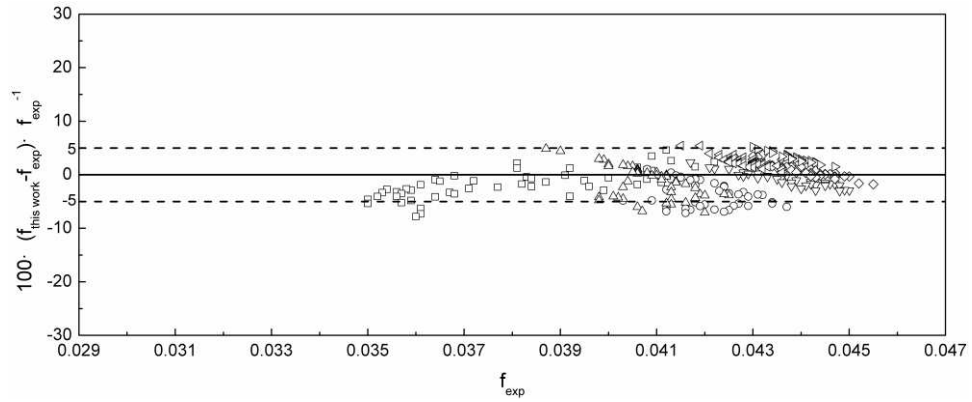
3 Figure 11 The deviation between the experimental friction factor ( $f_{exp}$ ) and (a) the calculated friction  
 4 factor which is obtained through Blasius equation ( $f_{Blasius}$ ), (b) the calculated friction factor which is  
 5 obtained through Moody equation ( $f_{Moody}$ ) for all the 538 data points in turbulent flow region, ■,  
 6 SS1011, ●, PEEK530, ▲, PEEK260, ▼, PEEK140.5, ◆, FS256, □, SS776, ○, SS523, △, SS526, ▽,  
 7 SS279, ◇, SS255, ◁, SS263, ▷, SS261. (SS, FS, PEEK stand for stainless steel, fused silica, and  
 8 poly-ether-ether-ketone, respectively, the number stands for the diameter of tested microtube)

9

10

11

12



1  
 2 Figure 12 The deviation between the experimental friction factor ( $f_{exp}$ ) and the calculated friction  
 3 factor which is obtained through the extended Moody equation (equation 22) ( $f_{this\ work}$ ) for the 304 data  
 4 points in turbulent flow region of rough microtubes,  $\square$ , SS776,  $\circ$ , SS523,  $\triangle$ , SS526,  $\nabla$ , SS279,  $\diamond$ ,  
 5 SS255,  $\triangleleft$ , SS263,  $\triangleright$ , SS261. (SS, FS, PEEK stand for stainless steel, fused silica, and  
 6 poly-ether-ether-ketone, respectively, the number stands for the diameter of tested microtube)